Comparative study of CPTU and SDMT in liquefaction prone silty sands with ground improvement

Sara Amoroso[1], Maria F. García Martínez[2], Paola Monaco[3], Laura Tonni[4], Guido Gottardi[5], Kyle M. Rollins[6], Luca Minarelli[7], Diego Marchetti[8], Kord J. Wissmann[9]

Abstract: Following the 2012 Emilia-Romagna seismic sequence, widespread liquefaction of silty sands was observed, providing the opportunity to enhance our knowledge of the influence of fines content on seismic hazard and mitigation works. This paper presents the results of a thorough geotechnical investigation performed in connection with full-scale controlled blast tests in Bondeno, a small village that suffered liquefaction in 2012. Piezocone (CPTU) and seismic dilatometer (SDMT) tests were performed in natural and improved soils after Rammed Aggregate Pier® (RAP) treatment to a depth of 9.5 m to provide accurate soil characterization, to evaluate liquefaction, and to verify the effectiveness of the ground improvement. The combined use of CPTU and DMT data provided reliable estimates of the overconsolidation ratio and at-rest earth pressure coefficient and highlighted the soil improvement in silty sands between 4 and 9 m in depth. Shear wave velocity measurements showed a low sensitivity to RAP installation. The treatment effectiveness was also confirmed by the use of the simplified procedures for liquefaction assessment, underlining the important influence of the adopted fines profile, and by the blast-induced liquefaction. CPTU and DMT parameters remained approximately unchanged between the piers after the detonation.

Keywords: controlled blasting, in-situ tests, liquefaction assessment, Rammed Aggregate Piers, silty sands, dense granular columns

INTRODUCTION

During the latest decades several "simplified procedures" for liquefaction assessment have been developed following the earthquakes and related co-seismic effects recorded around the world (e.g.,

[1] Assistant Professor, Department of Engineering and Geology, University of Chieti-Pescara, Viale Pindaro, 42, 65129 Pescara, Italy; Research Associate, Istituto Nazionale di Geofisica e Vulcanologia, Italy. ORCID: 0000-0001-5835-079X. Corresponding author, e-mail: sara.amoroso@unich.it
[2] Research Fellow, Department of Civil, Chemical, Environmental, and Materials Engineering, University of Bologna, Viale del Risorgimento, 2, 40136 Bologna, Italy. ORCID: 0000-0003-3965-5023.
[3] Associate Professor, Department of Civil, Architectural and Environmental Engineering, University of L'Aquila, Piazzale Ernesto Pontieri 1 – Monteluco di Roio, 67100 L'Aquila, Italy. ORCID: 0000-0002-1473-158X.
[4] Associate Professor, Department of Civil, Chemical, Environmental, and Materials Engineering, University of Bologna, Viale del Risorgimento, 2, 40136 Bologna, Italy. ORCID: 0000-0002-9391-6661.
[5] Full Professor, Department of Civil, Chemical, Environmental, and Materials Engineering, University of Bologna, Viale del Risorgimento, 2, 40136 Bologna, Italy. ORCID: 0000-0003-4944-8212.
[6] Full Professor, Department of Civil Environmental Engineering, Brigham Young University, 368 CB, Provo, UT 84602. ORCID: 0000-0002-8977-6619.
[7] Research Fellow, Istituto Nazionale di Geofisica and Vulcanologia, Viale Crispi, 43, 67100 L'Aquila, Italy. ORCID: 0000-0003-3602-9975.
[8] President and Chief Engineer, Studio Prof. Marchetti, Via Bracciano, 38, 00189 Rome, Italy. ORCID: 0000-0002-2544-3575.
[9] President and Chief Engineer, Geopier Foundation Company, 130 Harbour Place Drive, Suite 280, Davidson, NC 28036.

Seed and Idriss 1971, Robertson and Wride 1998, Andrus and Stokoe 2000, Youd et al. 2001, Idriss and Boulanger 2008, Kayen et al. 2013, Boulanger and Idriss 2014, Marchetti 2016, Saye et al. 2021). The use of these assessment approaches based on in-situ tests, such as the Standard Penetration Test (SPT), Cone Penetration Test (CPT), and shear wave velocity measurements (V_S) contemplates the application of a correction factor for the fines content (FC) of the soils susceptible to liquefaction. However, there is considerable uncertainty regarding the influence of non-plastic fines in relation to liquefaction triggering due to the cutoff value of the soil behavior type index (I_c) and the poor performance of I_c-FC correlations (specifically for CPT). In addition, uncertainty exists due to the presence of surface cohesive layers and/or interbedded plastic soils, and due to the assumption that the FC correction factors generally increase with increasing fines but are essentially "capped" at FC = 35% (e.g., Maurer et al. 2015a, Green et al. 2006, Prakash and Puri 2010, Polito and Martin 2001, Kokusho et al. 2012). These uncertainties require further study especially when applied to both natural and treated soils.

Several ground improvement solutions are available to mitigate the liquefaction hazard posed by clean sands, namely, increasing the soil resistance by densification or reducing the earthquake-induced excess pore pressures through drainage or reducing the shear strains through reinforcement. Vibratory compaction methods are a common and effective form of densification for cohesionless soils (Castro 1969), as proven by extensive research (e.g., D'Appolonia 1954, Mitchell 1981, Baez 1995, Adalier and Elgamal 2004, Wissmann et al. 2015, Vautherin et al. 2017 Amoroso et al. 2018). However, their effectiveness decreases as the fines content and plasticity increase (Mitchell 1981). Therefore, other ground improvement techniques, such as vibratory replacement, are often preferred in silty sands or sandy silts to protect the soil against liquefaction by increasing soil density, providing drainage for excess pore water pressures, and increasing the stiffness and shear resistance of the soil (Priebe 1998). Examples of this type of reinforcement include Stone Columns (SC), Soil Mixed Columns (SMC), and Rammed Aggregate Piers (RAP). This last approach appears to be a promising solution in sandy silts and silty sands to increase not only the density, but also the lateral stress and shear stiffness, which are often neglected and poorly understood (Smith and Wissmann 2018, Amoroso et al. 2020).

The at-rest earth pressure coefficient (K_0) is a key soil parameter that should be considered with reference to liquefaction mitigation works (Schmertmann 1985, Salgado et al. 1997, Harada et al. 2010). In this respect, in-situ tests have an essential role to play in estimating the horizontal stress in granular soils before and after treatment. As argued by Massarsch et al. (2019), the use of cone penetration test (CPT) and flat dilatometer test (DMT) results could produce improved estimates of K_0. Moreover, Baldi et al. (1986) and later Hossain and Andrus (2016) proposed a combined CPT-

DMT K_0-interpretation to take into account both the resistance and stress history of the soil, while the use of a CPT-only approach would have been overly affected by arching of stresses around the penetrating sleeve.

The coupling of CPT and DMT tests with down-hole geophysics (i.e., seismic piezocone SCPTU and seismic dilatometer SDMT) provides a more efficient approach to the task of geotechnical site characterization, offering clear opportunities for the economical and optimal collection of the data (Mayne et al. 2009). Therefore, direct push technologies are more relevant for understanding the changes in soil properties following ground improvement (e.g., Schmertmann et al. 1986, Jendeby 1992, Balachowski and Kurek 2015, Amoroso et al. 2018, Massarsch and Fellenius 2019), and the time-dependence of the soil properties following artificially induced-liquefaction, such as controlled blasting (e.g., Solymar 1984, Ashford et al. 2004, Finno et al. 2016, Amoroso et al. 2017, Passeri et al. 2018).

This investigation presents in-situ test results from a thorough geotechnical campaign performed before and after Rammed Aggregate Pier (RAP) treatment of a silty sand site in Bondeno (Italy). Bondeno is a small village strongly affected by liquefaction following the 2012 Emilia-Romagna seismic sequence where blast liquefaction testing was subsequently performed to understand the behavior of the treated soil relative to the untreated soil. The overall details of the research activities can be found in Amoroso et al. (2020) while details regarding the performance of the RAP group are provided by Rollins et al. (2021). This paper is focused on the results of piezocone (CPTU) and seismic dilatometer (SDMT) tests performed in natural and treated soils characterized by high non-plastic fines content, before and after blasting. These results provide accurate soil characterization, evaluate liquefaction potential, and verify the effectiveness of the ground improvement.

THE BONDENO TEST SITE (BTS)

Geological and geomorphological setting

The Bondeno Test Site (BTS) is located in the south-eastern portion of the Quaternary alluvial Po Plain, one of the largest and most populous plains in Europe. The area was affected in 2012 by an intense seismic activity linked to the tectonic evolution of the fault-fold structures (Fig. 1a) that form the front of the Apennine chain buried below the plain (e.g., Toscani et al. 2009).

The seismic sequence induced widespread site effects, including liquefaction manifestations, soil fracturing and lateral spreading (Emergeo Working Group 2013). These phenomena occurred mainly along ancient paleochannels (Fig. 1b) of the Po River and other minor rivers of Apennine origin (e.g., Civico et al. 2015, Caputo et al. 2016, Stefani et al. 2018), some of which preserve a strong morphological expression (Fig. 1c). The Quaternary evolution of these river systems led to the formation, in the subsoil, of a complex twist of elongated sandy deposits or paleochannels,

laterally confined by clayey deposits accumulated into interfluvial depression (e.g., Amorosi et al. 2016, Stefani et al. 2018). These continental sediments form the subsoil for a few hundred meters.

At BTS the liquefaction hazard is concentrated in a subsurface sandy deposit of a Holocene Po meander (Figs. 1c and 1d). Fig. 1c shows the higher elevations (brownish zones) indicating fluvial ridges bounding the lower, relatively flat interfluvial depression (greenish zones). The meandering course of the paleochannel is built up within the interfluvial depression and supports the identification of the paleochannel axis together with the location of sand boils. The meander base is frequently cut into upper Pleistocene coarse sand, accumulated during syn-glacial times. The meander unit geometry has been reconstructed through the analysis of remote sensing data (satellite images and LIDAR) and correlation of subsurface geotechnical investigations (Amoroso et al. 2020). This meander sand body is partially buried by finer grained levee sediment of historic age.

Site investigations

At the BTS the geotechnical campaign was structured in three phases, as detailed in Table 1 and Fig. 2, following the activities of the blast experimental research program, as described in general by Amoroso et al. (2020):

- Phase I consisted of site investigations performed before the treatment (pre-RAP) and before the blast (pre-blast). Boreholes with SPTs and disturbed soil sampling, CPTUs, and SDMTs were executed up to a maximum depth of 20 m in two relatively small circular areas (10 m-diameters at 20 m-spacing) associated with the blast experiment, one for testing the natural soil (Natural Panel, NP) and one for testing the improved soil (Improved Panel, IP). The aims were to verify the subsoil homogeneity, and to provide detailed geotechnical characterization and liquefaction assessment of the two blast panels;
- Phase II included site investigations carried out approximately one month after the pier installation (post-RAP) and before the blast (pre-blast) within the IP. The treatment consisted of a 4 × 4 quadrangular grid (2 m center-to-center spacing) of RAP columns, each 9.5 m long and with a final diameter of 0.5 m (area replacement ratio equal to 5%). Details regarding the construction methodology itself are reported in Saftner et al. (2018). Each CPTU, Medusa DMT (automated dilatometer test, see Marchetti et al. 2019) and SDMT test was performed up to a maximum depth of 15 m at the exact center between of four RAPs (see Fig. 2) to verify the effectiveness of the ground improvement technique especially regarding liquefaction;
- Phase III comprised three different site campaigns executed soon after the blast-induced liquefaction (post-blast June), then approximately two and three months after the controlled blasting (post-blast July and September) within the IP and NP. Details regarding the blast experiment are summarized in the next section. CPTU, Medusa DMT and SDMT tests were

carried out to a maximum depth of 15 m, and for the IP, the in-situ tests were located at the exact center between four RAPs (see Fig. 2). The goal of this phase was to study the time-dependence of soil properties following artificially induced-liquefaction both in the natural and treated soils.

Blast test experiment

To provide a direct comparison of ground performance with and without RAP treatment, blast liquefaction testing (Ashford et al. 2004) was performed at each test panel. A total of 16 explosive charges (8 of 0.5 kg at 3.5 m and 8 of 2.0 kg charges at 6.5 m in depth) were detonated sequentially at one second intervals around the periphery of two 10 m-diameter circles at each test panel. This blasting sequence induced liquefaction (excess pore pressure ratio R_u = 100%, where R_u is the ratio between the excess pore pressure and the effective vertical stress) to a depth of 11 m in the NP, but only induced R_u values of about 75% in the IP (Rollins et al. 2021). Ground surface settlement at the center of the NP was 10 cm, but only 4 cm in the IP. Based on profilometer measurements, settlement within the treated zone (0 to 9.5 m) was reduced by 75% in the IP relative to the NP (Pesci et al. 2022). Several large sand boils developed within the NP after blasting and produced considerable sand ejecta, while sand boils only developed outside the treated area in the IP (Amoroso et al. 2020). Thus, based on the metrics of excess pore pressure, settlement, and ejecta, the RAP group installation improved the site considerably.

SITE CHARACTERIZATION

First phase: initial conditions of natural ground

During the pre-RAP and pre-blast phase a borehole (S01), along with six SPTs, was carried out within the IP and 20 disturbed soil samples were extracted. The borehole log revealed the presence of a silty clay (CL) crust in the upper 3.5 m with an average plasticity index (*PI*) of 20%, followed by a non-plastic silty sand with *FC* typically in the range 25-35% and therefore classified as SM (Table 2), according to the Unified Soil Classification System, USCS (ASTM D2487-11 2011, ASTM D2488-09 2009).

A selection of grain size distribution curves determined on the soil samples is provided in Fig. 3a, whereas the SPT blow counts N_{SPT} recorded in silty sands are plotted in Fig. 3b, together with values of fines content obtained from sieve analysis. It is worth observing that results from particle size analysis are in good agreement with the high *FC* detected for the non-plastic silty-sandy deposits previously investigated in the liquefied areas after the 2012 Emilia-Romagna seismic sequence (e.g., Porcino and Diano 2016, Facciorusso et al. 2016, Fontana et al. 2019). SPT blow counts (N_{SPT}) turned out to be quite low between 3.5 and 6.0 m in depth, while increasing at greater depth. This preliminary information suggests a higher susceptibility to liquefaction in the upper part

of the SM layer.

Fig. 4a shows the profiles of the corrected cone resistance, q_t, sleeve friction, f_s, and pore pressure, u, obtained from two representative piezocone tests, namely CPTU11 and CPTU01, both carried out in the pre-RAP phase and located in the natural panel and in that to be treated, respectively. As detailed in the following, classification results and CPTU-based estimates of several relevant geotechnical parameters are also shown in Fig. 4a.

The comparative analysis of the q_t, f_s and u profiles reveals substantial agreement between the piezocone measurements collected in the two panels, thus indicating negligible horizontal spatial variability in the stratigraphic conditions of the whole test site. In particular, the interpretation of piezocone data in terms of the well-known classification framework by Robertson (2009), expressed as soil behavior type index (I_c), shows that most of the soils between 1.5 and 3.3 m in depth belong to the domains of silty clay/clayey silts. Compared to the natural panel, a slightly higher occurrence of silty sediments is observed in the panel selected for treatment. The underlying sediments, from 3.3 to 20 m, can be classified in both panels as predominantly silty sands. The I_c profiles computed from CPTU01 and CPTU11 are almost identical and generally oscillate about an average value equal to 1.75±0.10 and 1.77±0.12, respectively. However, the analysis of the pore pressure profile in the NP seems to suggest the presence of an interbedded layer of dilative silts at approximately 12.5-13.5 m in depth, not identified by the I_c. The latter is actually based only on the stress-normalized cone resistance Q_t and friction ratio F_r.

It is also worth observing that the application of a number of well-known CPTU-based empirical correlations (Robertson and Wride 1998, Suzuki et al. 1998, Boulanger and Idriss 2014), all dependent in different ways on the I_c, typically results in significant underestimation of the fines content, compared to the values obtained from grain size analysis. Indeed, as shown in Fig. 4a, good agreement with the average profile of laboratory *FC* is observed for the Boulanger and Idriss (2014) correlation for cohesive layer only.

Sands detected from 3.3 to 20 m in depth turn out to be in a medium-dense state. Most of the computed values of the relative density D_R, obtained by applying the correlation of Jamiolkowski et al. (2001) to the CPTU data, oscillate in the range of 50 to 60%. This outcome is also confirmed by discrete SPT-based predictions (Skempton 1986), which have been superimposed on the CPTU-based D_R profiles reported in Fig. 4a. According to the correlation developed by Robertson (2010), the corresponding state parameter ψ (as defined by Been and Jefferies 1985) has been found to be negative, on average close to -0.1 (thus theoretically suggesting dilative behavior at large strains), with minor differences over the whole thickness of the sandy layer. However, it is well-known that the determination of the in-situ soil state from cone penetration measurements actually involves

194 solving an inverse problem based on various independent geotechnical variables (Jefferies and Been
195 2006), hence the estimates of ψ provided by simplified relationships, such as those reported in Fig.
196 4a, must be seen as an approximation of the actual in-situ soil state and should therefore be
197 considered relatively uncertain.

198 The profile of the one-dimensional constrained modulus *M,* obtained by applying the empirical
199 correlation developed by Robertson (2009) in the framework of a so-called unified approach, shows
200 minor variations in the shallow silty clays and then increases with depth (approximately linearly) in
201 the underlying sands. These estimates cannot be compared for validation with any oedometer test
202 result, nor with compressibility parameters back-calculated from 1D field settlements. However, as
203 will be discussed subsequently, the *M* profile plotted in Fig. 4a turns out to be in a rather good
204 agreement with that computed from SDMT measurements. At the same time, it should be
205 mentioned that the application of other well-known CPTU-based correlations, either devised for
206 sands (e.g., Lunne and Christophersen 1983) or for silty sediments (e.g., Senneset et al. 1988),
207 resulted in predictions of *M* equal to about half the values provided by Robertson's unified
208 approach.

209 With regards to the soil shear strength of the sands, predictions of the effective peak friction
210 angle ϕ' provided by the Kulhawy and Mayne (1990) correlation appear to be in good agreement
211 with those computed from SPT blow counts. The profile exhibits minor variability from 3.3 to 20 m
212 in depth, with ϕ' estimates being on average equal to 37.7°±1.0° in the natural panel and 38.0°±0.9°
213 in the panel to be treated.

214 Fig. 4b summarizes the results obtained from SDMT in natural soils, in terms of profiles with
215 depth both of measured parameters, namely, the corrected DMT pressure readings p_0, p_1, p_2 and the
216 shear wave velocity V_S, along with parameters obtained from the usual DMT interpretation
217 (Marchetti 1980, Marchetti et al. 2001), namely, the material index I_D (indicating soil type), the
218 pore pressure index U_D (related to soil permeability), the horizontal stress index K_D (related to stress
219 history), the constrained modulus *M*, the friction angle ϕ' in sand, as well as the small strain shear
220 modulus G_0 obtained as $G_0 = \rho V_S^2$ (where ρ is the soil density, derived from the unit weight γ
221 estimated from DMT).

222 The values of p_0 and p_1 measured in the NP and IP (pre-RAP), as well as the derived
223 parameters, are generally similar or slightly variable, reflecting a general consistency of the soil
224 properties across the test area, as also observed from CPTU measurements. Below a depth of about
225 3.4 m, p_2 closely approximates the in-situ equilibrium pore pressure u_0 and accordingly $U_D \approx 0$,
226 indicating fully drained response, while in the upper soil layer $p_2 > u_0$ and $U_D > 0$, indicating
227 undrained response and excess pore pressure induced by blade penetration (Marchetti et al. 2001).

The interpretation of SDMT results, in particular I_D and U_D, are consistent with CPTU and borehole data, and identify an upper silty clay to clayey silt unit extending to a depth of about 3.4 m from the ground surface, underlain by silty sand down to a depth of about 12.6 m, followed by sandy silt at depths between about 12.6 and 13.4 m, and then silty sand down to the maximum investigated depth of 15 m.

Below a shallow "crust" (more pronounced in the IP), the different K_D values in the sandy units (paleochannel of the Po River from 3.4 to 12.6 m, glacial braided Po River deposits below 13.4 m) may be related to their different geologic depositional environment. In contrast, the V_S increases consistently with the effective vertical stress in all soil units.

The values of ϕ' estimated from SDMT in sand (Marchetti 1997) are broadly in agreement with the values obtained from the CPTU. The values of M estimated from the SDMT (Marchetti 1980), similar to those derived from the CPTU (Robertson 2009, Fig. 4a), indicate higher compressibility of the upper cohesive unit, while the sands below 3.4 m in depth are significantly less compressible. While M refers to stiffness at "working strain" level (Marchetti et al. 2008), G_0, corresponding to stiffness at very small strains, increases gradually with depth, without sharp contrasts between different soil units.

Fig. 5 shows the stratigraphic arrangement of the subsoil beneath the test site area along a North-South cross-section, as deduced by the combined interpretation of borehole logs, SPT, CPTU, Medusa DMT and SDMT described above, all carried out before the RAP installation. Apart from a 0.8 m thick topsoil layer (CH, according to USCS), the following well-defined stratigraphic units, also reflecting their sedimentological framework, could be identified:

- a layer of silty clays (CL, according to USCS), from 0.8 to about 3.3-3.5 m in depth;
- a predominantly silty sand unit, approximately 9 m thick, attributable to Holocene alluvial deposits of the Po River paleochannel. Samples recovered from this unit can be generally classified as SM, having a FC typically in the range 25-35% (see Table 2). Thin layers of coarser sediments have been occasionally found;
- a thin layer of sandy silt (ML), from 11.8-12.6 to 13.0-13.4 m in depth (interfluvial deposits);
- sands-silty sands (SP-SM) of the late Pleistocene epoch (namely, glacial braided Po River deposits), detected below 13.0-13.4 m in depth.

In this stratigraphic section, the groundwater table (GWT) is located at approximately 0.5 m from the ground surface, being governed by the water level in a nearby channel.

As evident from Fig. 5, the whole set of site investigations did not provide any significant evidence of horizontal spatial variability in the stratigraphic arrangement of the entire study area. Accordingly, the subsoil of the two panels appears to be fully comparable, and thus perfectly

suitable for analyzing the different responses of treated and untreated soils both during the blast test and some months after the liquefaction experiment.

Second phase: post-RAP treatment

Fig. 6 provides a comparison between field soil properties before and after RAP installation in the IP, in terms of both CPTU and SDMT profiles.

As regards the piezocone profiles, the increase in the q_t values after column construction appears to be particularly noticeable (q_t = 13.10 ± 1.76 MPa versus 9.54 ± 1.37 MPa before installation) from 6 to 8.5 m in depth, and relatively moderate from 4 to 6 m. Negligible changes in the q_t profile can be observed in the silty sands below the base of the piers. Obviously, these changes in q_t affect the computed estimates of the geotechnical parameters reported in Fig. 6, namely M, ψ, D_R and ϕ', as discussed below. The RAP treatment did not produce any improvement in the cohesive upper 4 m of the profile. This is consistent with experience in cohesive soils using other vibratory ground improvement techniques (Mitchell 1981).

The effect of RAP installation is evidently reflected by the increase in K_D (on average 48-53%), and even more in M from SDMT (80-87%), at depths between 4 and 9 m (Fig. 6, Table 3). The corresponding average increase in q_t is 30-35%. These results point to a significant increase in horizontal stress and stiffness resulting from pier installation, in agreement with previous observations (Saftner et al. 2018). In fact, the horizontal stress strongly influences both K_D and M estimated from the DMT using the Marchetti (1980) correlation, which incorporates K_D. The increase in M estimated from the CPTU is less pronounced, thus suggesting a lower sensitivity of q_t to an increase in horizontal stress. Between 6 and 8.5 m in depth, the pier installation increased D_R by an average of 10%, corresponding to a variation in the state parameter ψ of approximately -0.05 (more dilative), as deduced from CPTU measurements. Despite the uncertainties surrounding the computation of ψ, already mentioned, the computed trend is consistent with the increased density of the sand induced by RAP installation. As in the case of the CPTU, the SDMT did not any show significant improvement between 0 and 4 m in depth.

The observed results are in line with previous comparisons of pre- vs. post- CPTs and DMTs executed for monitoring ground improvement (e.g., Schmertmann et al. 1986, Jendeby 1992), since the RAP installation produced an average increase in M from DMT after treatment approximately 2.5 times the corresponding increase in cone penetration resistance q_c.

The decrease in K_D observed in the upper crust may be due in part to the construction of an overlying working platform, but also to the RAP installation under low confining stress and to seasonal variations in water content caused by the fluctuation of the GWT from 1.5 m (February 2018) to 0.5 m (March 2018), as reported in Table 1. No improvement was detected in the silty

sands below the toe of piers, unlike RAP case histories in clean sands studied in New Zealand (e.g., Wissmann et al. 2015, Vautherin et al. 2017).

To investigate further the variation of M before and after treatment in relation to data sources and computation methods, Fig. 7 shows a comparison between profiles of M computed by applying different empirical correlations (Robertson 2009, Lunne and Christophersen 1983, Senneset et al. 1988) to CPTU measurements, and estimates of M obtained from the SDMT (Marchetti 1980), in both natural and treated soils (IP pre- and post-RAP). For useful comparison, Fig. 7 also includes a few approximate values of M inferred from the SDMT-based small strain shear modulus G_0, assuming a conventional decay of G/G_0 at "working strain" level, namely $G/G_0 = 0.4$ (Gajo and Muir Wood 1999), together with a Poisson's ratio $\upsilon = 0.2$. In natural soils, M from the DMT is similar to M estimated from the CPTU when the Robertson (2009) correlation is adopted, while the M values provided by the alternative approaches (Lunne and Christophersen 1983, Senneset et al. 1988) turn out to be significantly lower. In treated soils, as mentioned, M values from the DMT show a more significant increment with respect to CPTU, thus confirming that the DMT is more sensitive to stiffness variations as a reasonable consequence of the increase of horizontal stress - and therefore of mean stress - produced by pier installation.

The combined interpretation of CPTU and DMT data provided information on the stress history and the state parameter in sand, in both the natural and treated soils as shown in Fig. 8. Filtering the data for $I_D \geq 1.8$ and $I_c \leq 2.6$, in the sandy layers the ratio M/q_t (with M estimated from DMT) is shown in Fig. 8. The average values of M/q_t are about 7-10 in natural soil and 13-14 in treated soil (Table 3). These values are in line with the available experience from field observations before and after compaction of sand fills, reported by Marchetti et al. (2001) and Marchetti and Monaco (2018), which show an increase in the ratio M from DMT to q_c from CPTU of between 5-10 before compaction to between 12-24 after compaction. The finding that compaction increases both M from DMT and q_c, but M at a faster rate, suggested the potential use of the ratio M from DMT/q_c, as a broad indicator of "equivalent" OCR in sands.

The in-situ earth pressure coefficient K_0 was estimated using correlations proposed by Baldi et al. (1986), based on both DMT and CPT data, and by Hossain and Andrus (2016), which require as an additional input also OCR (in this case evaluated according to Monaco et al. 2014). In the upper silty clay layer OCR and K_0 were estimated from the DMT (Marchetti 1980).

The OCRs of about 1-2 estimated in the natural soil, excluding the shallow "crust", indicate that the deposit is normally consolidated or slightly overconsolidated, with $K_0 \approx 0.5$-0.7. As an effect of the RAP installation, the "equivalent" OCR increased to about 3-3.5 and K_0 to about 0.9-1. The values of K_0 estimated according to Hossain and Andrus (2016) are lower than those estimated

according to Baldi et al. (1986). The increase of M/q_t, OCR and K_0 after treatment was more pronounced at depths between 7 and 9 m (Table 3).

An approximate estimate of the in-situ state parameter ψ in sand from DMT was obtained according to Yu (2004), with K_0 determined by both Baldi et al. (1986) and Hossain and Andrus (2016) methods. Fig. 8 shows that the input K_0 has a large influence on the calculated values of ψ, with an apparent contradiction versus the expected trend. In fact, the higher K_0 (i.e., higher OCR) estimated according to Baldi et al. (1986) should involve lower negative values of ψ compared to those obtained using K_0 from Hossain and Andrus (2016), while the opposite is observed in Fig. 8. On the other hand, the reduction of ψ after treatment found using both K_0 methods is consistent with the corresponding increase of OCR and K_0 before and after treatment. However, the computed values turn out to be significantly different from those obtained from CPTU data interpretation.

Third phase: post-blast conditions

Fig. 9 summarizes the results obtained from CPTU and SDMT pre- and post-blast. In the NP (Fig. 9a) the pre-blast data refer to natural soil, while in the IP (Fig. 9b) both to natural and treated soils. In both panels the post-blast data were collected immediately after the blast (June 2018), about one month later (July 2018), and about three months later (September 2018).

With regards to the piezocone tests in the NP, comparison between the pre-blast test (CPTU11) and that performed a few days after blasting (CPTU11ter) does not reveal any significant changes in soil response, in terms of q_t and the relevant parameters M, ψ, D_R, ϕ'. In addition, in spite of a somewhat horizontal spatial variability detected in tests conducted some months after the experiment (CPTU11quater and CPTU11quintus), only a slight increase in q_t can be observed from approximately 6.7 to 8.8 m. Consequently, little variation in M, ψ, D_R and ϕ' can be noticed within this depth interval. With respect to the CPTU tests in the IP, field measurements collected soon after and some months after the blast experiment show properties very similar to those observed in the post-RAP test (CPTU01bis). As a result, relevant changes in the predicted soil parameters cannot be clearly recognized from tests during the third-phase.

In natural soil (NP) the parameters K_D and M from DMT show an increase greater than 100% soon after the blast at depths between about 6 and 9 m, that can be related to the blast-induced settlements measured by the profilometer in the same depth interval (Rollins et al. 2021). However, these parameters remain unchanged at greater depths. An increase in these properties is also observed in the upper silty clay layer. In the following three months of observation, K_D and M from DMT do not exhibit any significant time-dependent gain or reduction overall, apart from local variations. In the treated soil (IP), the variation of K_D and M from DMT before and after the blast is much lower, possibly as a consequence of the effectiveness of the piers.

In both natural and treated soils V_S does not show changes before and after blasting, as previously found by Passeri et al. (2018) in another controlled blasting test performed in the natural silty sand of Emilia-Romagna.

LIQUEFACTION ASSESSMENT

Liquefaction assessment was performed in pre-blast natural (NS) and treated (TS) soils to verify the effectiveness of the RAP piers. The simplified procedure by Seed and Idriss (1971) has been applied to SPT, CPTU, DMT and V_S data, giving emphasis to the use of different in-situ test methods to provide a more reliable estimation as recommended by many authors (e.g., Robertson and Wride 1998, Youd and Idriss 2001, Idriss and Boulanger 2004). In particular, the cyclic resistance ratio at $M_w = 7.5$ ($CRR_{7.5}$) was evaluated by:

- the corrected SPT blow count $(N_1)_{60}$ obtained from Youd et al. (2001), Idriss and Boulanger (2008) and Boulanger and Idriss (2014) SPT-approaches and based on measured hammer energy;
- the normalized overburden corrected cone tip resistance q_{c1N} calculated from Robertson and Wride (1998), Idriss and Boulanger (2008) and Boulanger and Idriss (2014) CPTU-methods;
- the horizontal stress index K_D estimated from Monaco et al. (2005), Tsai et al. (2009), Robertson (2013) and Marchetti (2016) DMT-methods;
- the combination of q_{c1N} and K_D parameters into Marchetti (2016) CPTU-DMT correlation;
- the overburden stress corrected shear wave velocity V_{S1} in the Andrus and Stokoe (2000) and Kayen et al. (2013) V_S-based procedures.

To screen out "clay-like" soils, a threshold was set at $I_c \leq 2.6$ for CPT data and at $I_D \geq 1.0$ for DMT and V_S measurements, considering the non-plastic behavior of the silty sands, as provided by the Atterberg limits (Table 2). Due to the nature of the analyzed soil deposits, the application of a correction factor for the fines content was also contemplated for the liquefaction susceptibility: for SPT, CPTU and V_S methods the FC profile obtained from laboratory tests (namely "FC_{Lab}") was used (see Fig. 4a), while for DMT approaches, no FC corrections are available yet. Moreover, only for CPTU, liquefaction assessment was carried out also referring to the FC estimation of their own methods (see Fig. 4a; please note that the average curve from Suzuki et al. 1998 is the FC correlation used for the method by Idriss and Boulanger 2008 and that the fitting parameter C_{FC} was assumed equal to the default and average value, $C_{FC} = 0.0$, for Boulanger and Idriss 2014).

The cyclic stress ratio at $M_w = 7.5$ ($CSR_{7.5}$) was evaluated using two different seismic inputs:

- 2012 Emilia-Romagna earthquake: the epicenter of the main shock occurred on the 20th May 2012 was the closer at BTS, generating liquefaction evidences (Pizzi and Scisciani 2012) and recording a moment magnitude M_w = 5.9 (http://terremoti.ingv.it/en) and a peak ground

acceleration a_{max} = 0.29g (http://shakemap.rm.ingv.it/shake/index.html). The ShakeMaps were produced by the Istituto Nazionale di Geofisica e Vulcanologia and were previously used for liquefaction studies in the Emilia-Romagna area (Facciorusso et al. 2015, Santucci de Magistris et al. 2014);

- design earthquake: according to the ongoing seismic microzonation study of the Bondeno municipality and to the Italian Building Code (2018), the ground motion for a return period of 475 years corresponds to M_w = 6.14 and a_{max} = 0.22g.

Moreover, for SPT, CPTU and V_S methods the magnitude scaling factor (*MSF*) and the shear stress reduction coefficient (r_d) were evaluated according to the respective formulas provided by each method, while DMT approaches referred to the correlations by Idriss and Boulanger (2008). Finally, the GWT was assumed equal to 0.5 m, considering the most safe value estimated by CPTU and SDMT during the site investigations (Table 1).

Figs. 10 and 11 provide the results of the liquefaction analysis for natural (NS) and treated (TS) soils, respectively, using the 2012 Emilia-Romagna earthquake: the profiles of the liquefaction safety factor (FS_{liq}) and liquefaction potential index (*LPI*) according to Iwasaki et al. (1982) are shown for all the in-situ test methods, while the liquefaction induced vertical settlements (*S*) are plotted only for CPTU using Zhang et al. (2002). The main findings are listed below:

- the main liquefiable layer was confined approximately between 3.4 and 5.6 m according to most of the SPT and CPT methods (Figs. 10a and 10b), while it was limited on average from 3 to 4 m for DMT and V_S data due to the high values of K_D and V_S at greater depths (Figs. 10c and 10d);
- for the natural soil the *LPI* was generally $\leq$ 5 identifying a low liquefaction risk (Fig. 10), although the 2012 earthquake generated sand boils covering an area of about 4 to 6 meters length and 1.5 meters width. The lowest *LPI* values were obtained from (1) all the DMT and CPTU-DMT procedures, probably due to the smaller thickness detected for the liquefiable layer, (2) the SPT-approaches by Youd et al. (2001) and Idriss and Boulanger (2008) and (3) the CPTU-correlation by Idriss and Boulanger (2008) applying the laboratory *FC* profile. On the contrary, Boulanger and Idriss (2014) provided high and very high liquefaction risk for CPTU-based methods (assuming C_{FC} = 0.0), respectively;
- pre-RAP CPTU liquefaction analyses results were very sensitive to the non-plastic fines contents (Fig. 10b), confirming evidences already available in the international literature (e.g., Maurer et al. 2015a, Green et al. 2006, Prakash and Puri 2010, Polito and Martin 2001, Kokusho et al. 2012): the use of the *FC* profile from lab testing dramatically reduced ($\approx$ 70-80%) *LPI* and *S* estimated using a "blind" *FC* profile (i.e., the *FC* profile suggested by the various empirical methods – applied without the availability of soil sampling). Consequently,

the use of these laboratory data produced an underestimated result for Idriss and Boulanger (2008) and a more realistic liquefaction evaluation for Boulanger and Idriss (2014);

- for the post-RAP susceptibility assessment, the CPTU highlighted the effectiveness of the liquefaction mitigation treatment, showing a reduction of the *LPI* and *S* from 40 to 60% (Fig. 11a). In contrast, the decrease was not evident for DMT data (Fig. 11b), where, despite the consistent increase of the K_D and *M* values and of the CPTU-DMT combined parameters due to the piers (Figs. 6, 7 and 8, Table 3), the thin liquefiable layer between 3 and 4 m maintained a similar potential before and after treatment. The V_S measurements also did not provide a *LPI* decrease (Fig. 11c) that can be attributed to the absence of a significant increase in the shear wave velocity along the RAP length (Fig. 6, Table 3).

Following the above considerations, Table 4 shows liquefaction severity indices obtained for both the seismic inputs referring only to the CPTU data: beside the *LPI* and *S* already introduced, the Ishihara inspired liquefaction potential index (LPI_{ish}) according to Maurer et al. (2015b), and the liquefaction severity number (*LSN*) according to van Ballegooy et al. (2014) are reported. For the calculation of the LPI_{ish} the non-liquefiable crust was assumed to have a thickness of approximately 3.4 m, as provided by the CPTU profiles. All the indices evidenced a marked reduction comparing pre-RAP and post-RAP results, and an important influence of the adopted *FC* profile, as already emphasized. However, the LPI_{ish} and *LSN* values strongly underestimated the 2012 liquefaction evidences, while the *LPI* and *S* appeared to be closer to predicting what actually happened in Emilia-Romagna although still a little low. The design earthquake results underlined a similar trend when compared with the liquefaction indices obtained using the 2012 seismic input, even though the absolute values were smaller.

CONCLUSIONS

At the BTS a comprehensive comparative study based on CPTU and SDMT testing was carried out at a liquefaction-prone silty sand site improved by Rammed Aggregate Piers and subjected to controlled blasting. The main outcomes are summarized, as follows:

- CPTU and SDMT tests revealed a good agreement in the geotechnical characterization of the site, detecting homogenous soil properties in both the natural and improved panels. The use of both CPTU and DMT provided better estimates of soil properties in sandy layers (e.g. *OCR*, K_0), that are usually not determinable by the use of a single type of in-situ test;
- the comparison of the in-situ tests performed pre-blast in natural and treated soils highlighted the effectiveness of the RAP treatment between 4 and 9 m in depth within silty sands. The increases in the DMT parameters following treatment were more pronounced relative to those obtained from the CPTU data (e.g., K_D increased ≈ 48-53%, *M* increased ≈ 80-87%, q_t increased

≈ 30-35%), thus suggesting a higher sensitivity of DMT to the increase in horizontal stress. On the contrary, the V_S measurements showed a very low sensitivity to the ground improvement. Moreover, the combined use of CPTU and DMT tests showed a significant increase of M/q_t and K_0 after treatment, supporting the use of the piers to increase the lateral soil stress and mitigate liquefaction;

- the controlled blasting induced, soon after the detonation, an increase greater than 100% for K_D and M in the deeper silty sand layer (6-9 m in depth) of the natural panel, that remained constant with time. No time-dependency was observed in the improved panel, where CPTU and DMT parameters maintained the same pre-blast values confirming the effectiveness of the piers relative to liquefaction. Lastly in this case, the V_S measurements did not indicate any significant change between pre- and post-blast results in either the natural or treated soils;
- the liquefaction assessments by different geotechnical and geophysical tests provided broad agreement in detecting the 2012 liquefied layer, although DMT- and V_S-based methods suggested a low liquefaction risk for the natural soil. Comparing pre-RAP and post-RAP results, all the liquefaction severity indices evidenced a marked reduction as a result of RAP treatment and an important influence of the adopted *FC* profile. However, the LPI_{ish} and *LSN* values strongly underestimated the 2012 liquefaction evidences, while the *LPI* and *S* appeared to provide a better prediction - although still a little low - of what actually happened in Emilia-Romagna;
- further studies are required to investigate the mechanisms that reduced liquefaction-induced settlements around the piers by using both advanced laboratory tests and numerical modeling.

DATA AVAILABILITY STATEMENT

Some or all data, models, or code that support the findings of this study are available from the corresponding author upon reasonable request. These data include in-situ and laboratory test results.

ACKNOWLEDGEMENTS

The study was primarily funded by Geopier® Foundation Company (Davidson, North Carolina, United States). A special thanks also to Releo s.r.l. (Ferrara, Italy) who provided the installation of the Rammed Aggregate Piers. The in-situ testing campaign was carried out by CIRI Edilizia e Costruzioni, University of Bologna, Italy under the research project TIRISICO ("Tecnologie Innovative per la riduzione del rischio sismico delle Costruzioni", Project no. PG/2015/ 737636, POR-FESR 2014-2020). Financial contributions to this research activity were provided by INGV-FIRB Abruzzo project ("Indagini ad alta risoluzione per la stima della pericolosità e del rischio

sismico nelle aree colpite dal terremoto del 6 aprile 2009"), by INGV-Abruzzo Region project ("Indagini di geologia, sismologia e geodesia per la mitigazione del rischio sismico", L.R. n. 37/2016), and by Alma Mater Studiorum – Università di Bologna within AlmaIdea research project (2017, Scient. Resp. Laura Tonni). Special thanks to Brigham Young University for contributing to the realization of the blast test experiment in terms of personnel and technical equipment; to Prof. Marco Stefani (University of Ferrara, Italy) for kindly sharing scientific information of the studied area; to Michele Perboni who kindly guested the experimental activities; to the Bondeno Municipality and to the Emilia-Romagna Region (Luca Martelli), who provided all the necessary support to realize the research in collaboration with the other local authorities.

REFERENCES

Adalier, K., and Elgamal, A. 2004. "Mitigation of liquefaction and associated ground deformations by stone columns." *Eng. Geol.*, 72(3-4), 275-291.

Amorosi, A., Bruno, L., Facciorusso, J., Piccin, A., and Sammartino, I. 2016. "Stratigraphic control on earthquake-induced liquefaction: a case study from the Central Po Plain (Italy)." *Sediment. Geol.*, 345, 42–53.

Amoroso, S., Rollins, K. M., Andersen, P., Gottardi, G., Tonni, L., García Martínez, M. F., Wissmann, K. J., Minarelli, L., Comina, C., Fontana, D., De Martini, P. M., Monaco, P., Pesci, A., Sapia, V., Vassallo, M., Anzidei, M., Carpena, A., Cinti, F. R., Civico, R., Coco, I., Conforti, D., Doumaz, F., Giannattasio, F., Di Giulio, G., Foti, S., Loddo, F., Lugli, S., Manuel, M. R., Marchetti, D., Mariotti, M., Materni, V., Metcalfe, B., Milana, G., Pantosti, D., Pesce, A., Salocchi, A. C., Smedile, A., Stefani, M., Tarabusi, G., and Teza, G. 2020. "Blast-induced liquefaction in silty sands for full-scale testing of ground improvement methods: insights from a multidisciplinary study." *Eng. Geol.*, 265, 105437. https://doi.org/10.1016/j.enggeo.2019.105437.

Amoroso, S., Milana, G., Rollins, K. M., Comina, C., Minarelli, L., Manuel, M. R., Monaco, P., Franceschini, M., Anzidei, M., Lusvardi, C., Cantore, L., Carpena, A., Casadei, S., Cinti, F. R., Civico, R., Cox, B. R., De Martini, P. M, Di Giulio, G., Di Naccio, D., Di Stefano, G., Facciorusso, J., Famiani, D., Fiorelli, F., Fontana, D., Foti, S., Madiai, C., Marangoni, V., Marchetti, D., Marchetti, S., Martelli, L., Mariotti, M., Muscolino, E., Pancaldi, D., Pantosti, D., Passeri, F., Pesci, A., Romeo, G., Sapia, V., Smedile, A., Stefani, M., Tarabusi, G., Teza, G., Vassallo, M., and Villani, F. 2017. "The first Italian blast-induced liquefaction test (Mirabello, Emilia-Romagna, Italy): description of the experiment and preliminary results." *Ann. Geophys.*, 60(5), S0556. https://doi.org/10.4401/ag-7415.

533 Amoroso, S., Rollins, K. M., Monaco, P., Holtrigter, M., and Thorp, A. 2018. "Monitoring ground
534 improvement using the seismic dilatometer in Christchurch, New Zealand." *Geotech. Test. J.*, 41
535 (5), 946–966. https://doi.org/10.1520/GTJ20170376.
536 Andrus, R. D., and Stokoe, K. H. II. 2000. "Liquefaction Resistance of Soils from Shear-Wave
537 Velocity," *J. Geotech. Geoenviron. Eng.*, 126(11): 1015–1025.
538 https://doi.org/10.1061/(ASCE)1090-0241(2000)126:11(1015).
539 Ashford, S., Rollins, K. M., and Lane, J. 2004. "Blast-induced liquefaction for full-scale foundation
540 testing." *J. Geotech. Geoenviron. Eng.*, 130(8): 798-806. https://doi.org/10.1061/(ASCE)1090-
541 0241(2004)130:8(798).
542 ASTM D2487-11. 2011. *Standard practice for classification of soils for engineering purposes*
543 *(Unified Soil Classification System)*. West Conshohocken, PA: ASTM International.
544 ASTM D2488-09. 2009. *Standard Practice for description and identification of soils (visual-*
545 *manual procedure).* West Conshohocken, PA: ASTM International.
546 Baez, J.I. 1995. *A design model for the reduction of soil liquefaction by vibrostone columns.* Ph.D
547 dissertation, Univ. of Southern California.
548 Balachowski, L., and Kurek, N. 2015. "Vibroflotation Control of Sandy Soils." In *Proc., 3rd Int.*
549 *Conf. on the Flat Dilatometer*, 185–190.
550 Baldi, G., Bellotti, R., Ghionna, V., Jamiolkowski, M., Marchetti, S., and Pasqualini, E. 1986. "Flat
551 dilatometer tests in calibration chambers." In *Proc., Specialty Conf. on Use of In Situ Tests in*
552 *Geotechnical Engineering GSP 6*, 431–446. Reston, VA: ASCE.
553 Been, K., and Jefferies, M. G. 1985. A state parameter for sands. *Géotechnique*, 35(2), 99–112.
554 Boulanger, R. W., and Idriss, I. M. 2014. *CPT and SPT based liquefaction triggering procedures*.
555 Rep. No. UCD/CGM-14/01. Davis, CA: Center for Geotechnical Modeling, Dept. of Civil and
556 Environmental.
557 Caputo, R., Poli, M. E., Minarelli, L., Rapti-Caputo, D., Sboras, S., Stefani, M., and Zanferrari, A.
558 2016. "Palaeoseismological evidence for the 1570 Ferrara earthquake, Italy." *Tectonics*, 35, 1423-
559 1445. https://doi.org/10.1002/2016TC004238.
560 Castro, G. 1969. *Liquefaction of sands.* Ph.D. Dissertation, Harvard University.
561 Civico, R., Brunori, C. A., De Martini, P. M., Pucci, S., Cinti, F. R., and Pantosti, D. 2015.
562 "Liquefaction susceptibility assessment in fluvial plains using airborne LIDAR: the case of the
563 2012 Emilia earthquake sequence area (Italy)." *Nat. Hazards Earth Syst. Sci.*, 15, 2473–2483.
564 D'Appolonia, E. 1954. "Loose sands - their compaction by vibroflotation." In *Proc., Symp. on*
565 *Dynamic Testing of Soils*, 138-162. West Conshohocken, PA: ASTM International.

566 Emergeo Working Group. 2013. “Liquefaction phenomena associated with the Emilia earthquake
567 sequence of May-June 2012 (Northern Italy).” *Nat. Hazards Earth Syst. Sci.*, 13 (4), 935–947.
568 Facciorusso, J., Madiai, C., and Vannucchi, G. 2015. “CPT-Based Liquefaction Case History from
569 the 2012 Emilia Earthquake in Italy.” *J. Geotech. Geoenviron. Eng.*, 141(12): 1032-1051.
570 https://doi.org/10.1061/(ASCE)GT.1943-5606.0001349.
571 Facciorusso, J., Madiai, C., and Vannucchi, G. 2016. “The 2012 Emilia earthquake (Italy):
572 geotechnical characterization and ground response analyses of the paleo-Reno river levees.” *Soil
573 Dyn. Earthq. Eng.*, 865, 71-88.
574 Finno, R.J., Gallant, A.P., and Sabatini, P.J. 2016. “Evaluating ground improvement after blast
575 densification at the Oakridge landfill.” *J. Geotech. Geoenviron. Eng.*, 142(1): 04015054.
576 https://doi.org/10.1061/(ASCE)GT.1943-5606.0001365.
577 Fontana, D., Amoroso, S., Minarelli, L., and Stefani, M. 2019. “Sand liquefaction phenomena
578 induced by a blast test: new insights from composition and texture of sands (late Quaternary,
579 Emilia, Italy).” *J. Sediment. Res.*, 89(1), 13-27, https://doi.org/10.2110/jsr.2019.1.
580 Gajo, A., and Muir Wood, D. 1999. “Severn-Trent sand: a kinematic-hardening constitutive model:
581 the q-p formulation.” *Géotechnique*, 49(5), 595–614.
582 Green, R. A., Olsen, S., and Polito, C. 2006. “A comparative study of the influence of fines on the
583 liquefaction susceptibility of sands: field versus laboratory.” In: *Proc., 8th U.S. Nat. Conf. on
584 Earthquake Engineering*. 14, 8229–8238. Oakland, CA: EERI.
585 Harada, K., Orense, R.P., Ishihara, K., and Mukai, J. 2010. “Lateral stress effects on liquefaction
586 resistance correlations.” *Bull. New Zeal. Soc. Earthq. Eng.*, 43(1), 13-23.
587 Hossain, M. A., and Andrus, R. D. 2016. “At-rest lateral stress coefficient in sands from common
588 field methods.” *J. Geotech. Geoenviron. Eng.* 142(12): 06016016.
589 https://doi.org/10.1061/(ASCE)GT.1943-5606.0001560.
590 Idriss, I. M., and Boulanger, R. W. 2004. “Semi-empirical procedures for evaluating liquefaction
591 potential during earthquakes.” In *Proc., 11th Int. Conf. on Soil Dynamics and Earthquake
592 Engineering and 33rd Int. Conf. on Earthquake Geotechnical Engineering*, 32-56. Singapore:
593 Stallion Press.
594 Idriss, I. M. and Boulanger, R. W. 2008. *Soil liquefaction during earthquakes*. Report No. MNO-
595 12. Oakland, CA: Earthquake Engineering Research Institute.
596 Italian Building Code (2018). *Norme tecniche per le costruzioni* [*Technical building regulations*].
597 [in Italian] Gazzetta Ufficiale n. 42/2017. Suppl. Ordinario n. 8.

598 Iwasaki, T., Tokida, K., Tatsuoka, F., Yasuda, S. and Sato, H. 1982. "Microzonation for soil
599 liquefaction potential using simplified methods." In Vol. 3 of *Proc., 3rd Int. Conf. on*
600 *Microzonation*, 1319-1330. Washington, DC: NSF.
601 Jamiolkowski, M., Lo Presti, D. C. F., and Manassero, M. 2001. "Evaluation of relative density and
602 shear strength of sands from cone penetration test and flat dilatometer test." In *Proc., Symp. on Soil*
603 *Behaviour and Soft ground Construction GSP 119*, 201-238. Reston, Virginia: ASCE.
604 Jefferies, M., and Been, K. 2006. *Soil Liquefaction. A critical state approach*. Taylor and Francis.
605 Jendeby, L. 1992. "Deep Compaction by Vibrowing." In Vol. 1 of *Proc.*, *Nordic Geotechnical*
606 *Meeting*, 19–24. Lyngby (Denmark): Danish Geotechnical Society.
607 Kayen, R., Moss, R. E. S., Thompson, E. M., Seed, R. B., Cetin, K. O., Der Kiureghian, A., Tanaka,
608 Y., and Tokimatsu, K. 2013. "Shear-wave velocity-based probabilistic and deterministic assessment
609 of seismic soil liquefaction potential." *J. Geotech. Geoenviron. Eng.*, 139(3): 407–419.
610 https://doi.org/10.1061/(ASCE)GT.1943-5606.0000743.
611 Kokusho, T., Ito, F., Nagao, Y., and Green, R. A. 2012. "Influence of non/low-plastic fines and
612 associated aging effects on liquefaction resistance." *J. Geotech. Geoenviron. Eng.*, 138(6): 747-756.
613 https://doi.org/10.1061/(ASCE)GT.1943-5606.0000632.
614 Kulhawy, F. H., and Mayne, P. W. 1990. *Manual on estimating soil properties for foundation*
615 *design*. Report No. EL-6800. Palo Alto, CA: Electric Power Research Institute (EPRI).
616 Lunne, T., and Christophersen, H. P. 1983. "Interpretation of cone penetrometer data for offshore
617 sands." In *Proc., 15th Annual Offshore Technology Conference*, 181-188.
618 Marchetti, D., Monaco, P., Amoroso, S., and Minarelli, L., 2019. "In situ tests by Medusa DMT."
619 In *Proc., XVII Eur. Conf. on Soil Mechanics and Geotechnical Engineering*,
620 https://doi.org/10.32075/17ECSMGE-2019-0657.
621 Marchetti, S. 1980. "In situ tests by flat dilatometer." *J. Geotech. Eng. Div.*, 106 (3): 299–321.
622 https://doi.org/10.1061/AJGEB6.0000934
623 Marchetti, S. 1997. "The flat dilatometer: design applications." In *Proc.*, *3rd Int. Geotech. Eng.*
624 *Conf.*, 421–448.
625 Marchetti, S. and Monaco, P. 2018. "Recent Improvements in the use, interpretation, and
626 applications of DMT and SDMT in Practice." *Geotech. Test. J.* 41 (5), 837–850.
627 https://doi.org/10.1520/GTJ20170386.
628 Marchetti, S. 2016. "Incorporating the stress history parameter K_D of DMT into the liquefaction
629 correlations in clean uncemented sands." *J. Geotech. Geoenviron. Eng.*, 142(2): 04015072.
630 https://doi.org/10.1061/(ASCE)GT.1943-5606.0001380.

631 Marchetti, S., Monaco, P., Totani, G. and Marchetti, D. 2008. "In situ tests by seismic dilatometer
632 (SDMT)." In *Proc., Symp. Honoring Dr. John H. Schmertmann for His Contributions to Civil*
633 *Engineering at Research to Practice GSP 180*, 292–311. https://doi.org/10.1061/40962(325)7.
634 Marchetti, S., Monaco, P., Totani, G., and Calabrese, M. 2001. "The Flat Dilatometer Test (DMT)
635 in Soil Investigations – A Report by the ISSMGE Committee TC16." In *Proc., 2nd Int. Conf. on the*
636 *Flat Dilatometer*, 7–48.
637 Massarsch, K. R., and Fellenius, B. H. 2019. "Evaluation of vibratory compaction by in-situ tests."
638 *J. Geotech. Geoenviron. Eng.*, 145(12): 05019012. https://doi.org/10.1061/(ASCE)GT.1943-
639 5606.0002166.
640 Massarsch. K. R., Wersäll, C., and Fellenius, B. H. "Horizontal stress increase induced by deep
641 vibratory compaction." *P. I. Civil Eng. Geotec.*, 173(3), 228-253.
642 Maurer, B. W., Green, R. A., Cubrinovski, M., and Bradley, B. A. 2015a. "Fines-content effects on
643 liquefaction hazard evaluation for infrastructure during the 2010-2011 Canterbury, New Zealand
644 earthquake sequence." *Soil Dyn. Earthq. Eng.*, 76, 58-68.
645 Maurer, B. W., Green, R. A., and Taylor, O. D. S. 2015b. "Moving towards an improved index for
646 assessing liquefaction hazard: lessons from historical data." *Soils Found.*, 55(4), 778–787.
647 Mayne, P. W., Coop, M. R., Springman, S. M., Huang, A. B. and Zornberg, J. G. 2009.
648 "Geomaterial behavior and testing." In Vol. 4 of *Proc., 17th Int. Conf. on Soil Mechanics and*
649 *Geotechnical Engineering*, 2777-2872.
650 Mitchell, J. K. 1981. "Soil improvement: state-of-the-art.", In Vol. 4 of *Proc., 10th Int. Conf. on Soil*
651 *Mechanics and Foundation Engineering*, 509-565.
652 Monaco, P., Amoroso, S., Marchetti, S., Marchetti, D., Totani, G., Cola, S., and Simonini, P. 2014.
653 "Overconsolidation and stiffness of Venice lagoon sands and silts from SDMT and CPTU." *J.*
654 *Geotech. Geoenviron. Eng.* 140 (1): 215–227. https://doi.org/10.1061/(ASCE)GT.1943-
655 5606.0000965.
656 Monaco, P., Marchetti, S., Totani, G., and Calabrese, M. 2005. "Sand liquefiability assessment by
657 flat dilatometer test (DMT)." In Vol. 4 of *Proc., XVI Int. Conf. on Soil Mechanics and Geotechnical*
658 *Engineering*, 2693-2697.
659 Passeri, F., Comina, C., Marangoni, V., Foti, S., and Amoroso, S. 2018. "Geophysical tests to
660 monitor blast-induced liquefaction, the Mirabello (NE, Italy) test site." *J. Environ. Eng. Geoph.*,
661 23(3), 319-333, https://doi.org/10.2113/JEEG23.3.319.
662 Pesci, A., Teza, G., Loddo, F., Rollins, K.M., Andersen, P., Minarelli, L., and Amoroso, S. 2022.
663 "Remote sensing of induced liquefaction: TLS and SfM for a full-scale blast test." *J. Surv. Eng.*,
664 148(1): 04021026. https://doi.org/10.1061/(ASCE)SU.1943-5428.0000379

Pizzi, A., and Scisciani, V. 2012. "The May 2012 Emilia (Italy) earthquakes: preliminary interpretations on the seismogenic source and the origin of the coseismic ground effects." *Ann. Geophys.*, 55(4), 751–757.

Polito, C. P., and Martin J. R. II 2001. "Effects of non-plastic fines on the liquefaction resistance of sands." *J. Geotech. Geoenviron. Eng.*, 127 (5): 408-415. https://doi.org/10.1061/(ASCE)1090-0241(2001)127:5(408)

Porcino, D., and Diano, V. 2016. "Laboratory study on pore pressure generation and liquefaction of low plasticity silty sandy soils during the 2012 earthquake in Italy." *J. Geotech. Geoenviron. Eng.*, 142(10): 04016048. https://doi.org/10.1061/(ASCE)GT.1943-5606.0001518

Prakash, S., and Puri, V. K. 2010. "Recent advances in liquefaction of fine grained soils." In *Proc., 5th Int. Conf. on Recent Advances in Geotechnical Earthquake Engineering and Soil Dynamics.* Rolla, Missouri: Missouri University of Science and Technology.

Priebe, H. J. 1998. "Vibro replacement to prevent earthquake induced liquefaction," *Ground Eng.*, 31(9), 30-33. UK: Emap Construct.

Robertson, P.K. 2010. "Estimating in-situ state parameter and friction angle in sandy soils from the CPT." In *Proc., 2nd Int. Symp. on Cone Penetration Testing*, 1-8. Madison WI: Omnipress.

Robertson, P. K. 2013. "The James K. Mitchell Lecture: Interpretation of in-situ tests – some insights." In Vol. 1 of *Proc., 4th Int. Conf. Geotechnical & Geophysical Site Characterization*, 3-24. London, UK: CRC Press / Taylor & Francis Group.

Robertson, P. K. and Wride, C. E. 1998. "Evaluating cyclic liquefaction potential using the cone penetration test." *Can. Geotech. J.*, 35(3), 442-459.

Robertson, PK. 2009. "Interpretation of cone penetration tests – a unified approach." *Can. Geotech. J.*, 46(11), 1337–1355.

Rollins, K. M., Amoroso, S., Andersen, P., Tonni, L., and Wissmann, K. J. (2021). "Liquefaction mitigation of silty sands using rammed aggregate piers based on blast-induced liquefaction testing." *J. Geotech. Geoenviron. Eng.*, 147(9): 04021085. https://doi.org/10.1061/(ASCE)GT.1943-5606.0002563

Saftner, D. A., Zheng, J., Green, R. A., Hryciw, R. and Wissmann, K. J. 2018. "Rammed aggregate pier installation effect on soil properties." *P. I. Civil Eng. Ground Impr.* 171 (2), 63–73.

Salgado, R., Boulanger, R. W., and Mitchell, J. K. 1997. "Lateral stress effect on CPT liquefaction resistance correlations." *J. Geotech. Geoenviron. Eng.*, 123(8): 726-735. https://doi.org/10.1061/(ASCE)1090-0241(1997)123:8(726)

Santucci de Magistris, F., Lanzano, G., Forte, G., and Fabbrocino, G. 2014. "A peak acceleration threshold for soil liquefaction: lessons learned from the 2012 Emilia earthquake (Italy)." *Nat. Hazards*, 74(2), 1069-1094.

Saye, S. R., Olson S. M., and Franke, K. W. 2021. "Common-Origin Approach to Assess Level-Ground Liquefaction Susceptibility and Triggering in CPT-Compatible Soils Using ΔQ." *J. Geotech. Geoenviron. Eng.*, 147(7): 04021046. https://doi.org/10.1061/(ASCE)GT.1943-5606.0002515

Schmertmann, J. H. 1985. "Measure and use of the in situ lateral stress." *The Practice of Foundation Engineering, A Volume Honoring Jorj O. Osterberg*, 189–213.

Schmertmann, J. H., Baker, W., Gupta, R., and Kessler, K. 1986. "CPT/DMT q_C of ground modification at a power plant." In *Proc., Specialty Conf. on Use of In Situ Tests in Geotechnical Engineering GSP 6*, 985–1001. Reston, VA: ASCE.

Seed, H. B. and Idriss, I. M. 1971. "Simplified procedure for evaluating soil liquefaction potential." *J. Geotech. Engrg. Div.*, 97(9): 1249–1273. https://doi.org/10.1061/JSFEAQ.0001662

Senneset, K., Sandven, R., Lunne, T., and Amundsen, T. 1988. "Piezocone Tests in Silty Soils." In Vol. 2 of *Proc., Int. Symp. on Penetration Testing*, 955-966. Rotterdam, The Netherlands: Balkema.

Skempton, A. W. 1986. "Standard penetration test procedures and the effects in sands of overburden pressure, relative density, particle size, aging and overconsolidation." *Geotechnique*, 36(3), 425-447.

Smith, M. E., and Wissmann, K. J. 2018. "Ground improvement reinforcement mechanisms determined for the Mw 7.8 Muisne, Ecuador, earthquake." In *Proc., 5th Geotechnical Earthquake Engineering and Soil Dynamics Conference: Liquefaction Triggering, Consequences, and Mitigation*, 286-294. Washington, DC: ASCE.

Solymar, Z. V. 1984. "Compaction of alluvial sands by deep blasting." *Can. Geotech. J.*, 21(2), 305–321.

Stefani, S., Minarelli, L., Fontana, A., and Hajdas, I. 2018. "Regional deformation of late Quaternary fluvial sediments in the Apennines foreland basin (Emilia, Italy)." *Int. J. Earth Sci.*, 107(7), 2433–2447. https://doi.org/10.1007/s00531-018-1606-x.

Suzuki, Y., Sanematsu, T., and Tokimatsu, K. 1998. "Correlation between SPT and seismic CPT." In Vol. 2 of *Proc., 1st Int. Conf. on Site Characterization*, 1375–1380. Rotterdam, The Netherlands: Balkema.

Toscani, G., Burrato, P., Di Bucci, D., Seno, S., and Valensise, G. 2009. "Plio-Quaternary tectonic evolution of the northern Apennines thrust fronts (Bologna-Ferrara section, Italy): seismotectonic implications." *Ital. J. Geosci.*, 128, 605–613.

731 Tsai, P., Lee, D., Kung, G. T. and Juang, C. H. 2009. "Simplified DMT-based methods for
732 evaluating liquefaction resistance of soils." *Eng. Geol.*, 103(2009), 13-22.
733 van Ballegooy, S., Malan, P., Lacrosse, V., Jacka, M. E., Cubrinovski, M., Bray, J. D., O'Rourke,
734 T. D., Crawford, S. A., and Cowan, H. 2014. "Assessment of liquefaction-induced land damage for
735 residential Christchurch." *Earthq. Spectra*, 30(1), 31–55.
736 Vautherin, E., Lambert, C., Barry-Macaulay, D., and Smith, M. 2017. "Performance of rammed
737 aggregate piers as a soil densification method in sandy and silty soils: experience from the
738 Christchurch rebuild." In *Proc., 3rd Int. Conf. on Performance-based Design in Earthquake*
739 *Geotechnical Engineering*. London, UK: ISSMGE.
740 Wentz, F. J., van Ballegooy, S., Rollins, K. M., Ashford, S. A., and Olsen, M. J. 2015. "Large scale
741 testing of shallow ground improvements using blast-induced liquefaction." In *Proc., 6th Int. Conf.*
742 *on Earthquake Geotechnical Engineering*. London, UK: ISSMGE.
743 Wissmann, K. J., van Ballegooy, S., Metcalfe, B. C., Dismuke, J. N., and Anderson, C. K. 2015.
744 "Rammed aggregate pier ground improvement as a liquefaction mitigation method in sandy and
745 silty soils," In *Proc., 6th Int. Conf. on Earthquake Geotechnical Engineering*. London, UK:
746 ISSMGE.
747 Youd, T. L., Idriss, I. M., Andrus, R. D., Arango, I., Castro, G., Christian, J. T., Dobry, R., Finn, W.
748 D. L., Harder, L. F. Jr., Hynes, M. E., Ishihara, K., Koester, J. P., Liao, S. S. C., Marcuson, W. F.,
749 Martin, G. R. II, Mitchell, J. K., Moriwaki, Y., Power, M. S., Robertson, P. K, Seed, R. B., and
750 Stokoe, K. H. II. 2001. "Liquefaction resistance of soils: summary report from the 1996 NCEER
751 and 1998 NCEER/NSF workshops on evaluation of liquefaction resistance of soils." *J. Geotech.*
752 *Geoenviron. Eng.*, 127(10): 817-833. https://doi.org/10.1061/(ASCE)1090-0241(2001)127:10(817)
753 Youd, T. L., and Idriss, I. M. 2001. "Liquefaction resistance of soils: summary report from the 1996
754 NCEER and 1998 NCEER/NSF workshops on evaluation of liquefaction resistance of soils." *J.*
755 *Geotech. Geoenviron. Eng.*, 127(4): 297-313. https://doi.org/10.1061/(ASCE)1090-
756 0241(2001)127:4(297)
757 Yu, H. S. 2004. "James K. Mitchell Lecture – In situ soil testing: from mechanics to interpretation."
758 In *Proc., 2nd Int. Conf. on Site Characterization*, 1, 3–38. London, UK: Taylor & Francis Group.
759 Zhang, G., Robertson, P. K., and Brachman, R. W. I. 2002. "Estimating Liquefaction Induced
760 Ground Settlements from CPT for Level Ground." *Can. Geotech. J.*, 39(5), 1168–1180.

Tables

Table 1. List of the in-situ tests associated with the different phases of the BTS experimental program: phase I is pre-RAP and pre-blast; phase II is post-RAP and pre-blast; phase III is post-blast. Ground water table (GWT) from each test is indicated.

Phase	*Period*	*Location*	*Borehole*	*CPTU test*	*DMT-SDMT test*	*GWT from CPTU test (m)*	*GWT from DMT test (m)*
I	February 2018	IP	S01	CPTU01	SDMT01	1.50	1.50
I	February 2018	NP	S11	CPTU11	-	1.50	-
I	March 2018	IP	-	CPTU02	MEDUSA DMT01	0.50	0.50
I	April 2018	NP	-	CPTU12	SDMT11	0.80	0.80
I	April 2018	Between IP-NP	-	-	MEDUSA DMT11	-	0.80
II	April 2018	IP	-	-	MEDUSA DMT01bis	-	0.80
II	April 2018	IP	-	CPTU01bis	SDMT01bis	0.85	0.80
III	June 2018	IP	-	CPTU01ter	SDMT01ter	0.70	0.70
III	June 2018	NP	-	CPTU11ter	SDMT11ter	0.80	0.70
III	July 2018	IP	-	CPTU01quater	SDMT01quater	0.60	0.80
III	July 2018	NP	-	CPTU11quater	SDMT11quater	0.64	0.80
III	September 2018	IP	-	CPTU01quintus	SDMT01quintus	0.90	0.43
III	September 2018	NP	-	CPTU11quintus	MEDUSA DMT11quintus	0.90	2.00
III	September 2018	NP	-	-	SDMT11quintus	-	-

Table 2. Index properties of the analyzed samples related to USCS soil classification.

Panel	*Depth (m)*	*FC (%)*	*PI (%)*	C_U *(-)*	C_C *(-)*	*USCS classification*
natural panel (NP)	3.30-3.50	88.24	17.6	-	-	Silty clay (CL)*
natural panel (NP)	3.60-3.80	22.64	non-plastic	-	-	Silty sand (SM)*
natural panel (NP)	4.30-4.50	40.79	non-plastic	-	-	Silty sand (SM)*
natural panel (NP)	5.50-5.70	22.44	non-plastic	-	-	Silty sand (SM)*
natural panel (NP)	6.80-7.00	26.02	non-plastic	-	-	Silty sand (SM)*
natural panel (NP)	7.00-7.10	30.81	non-plastic	-	-	Silty sand (SM)*
improved panel (IP)	2.15-2.30	82.02	22.1	-	-	Silty clay (CL)*
improved panel (IP)	2.80-3.00	92.63	21.6	-	-	Silty clay (CL)*
improved panel (IP)	3.30-3.50	75.25	-	-	-	Silty clay (CL)*
improved panel (IP)	4.35-4.50	28.24	non-plastic	-	-	Silty sand (SM)*
improved panel (IP)	4.50-4.95	20.50	non-plastic	-	-	Silty sand (SM)*
improved panel (IP)	5.45-5.60	20.45	non-plastic	17.23	4.11	Silty sand (SM)
improved panel (IP)	5.60-6.05	35.71	non-plastic	-	-	Silty sand (SM)*
improved panel (IP)	6.25-6.45	31.38	non-plastic	39.30	1.09	Silty sand (SM)
improved panel (IP)	7.40-7.50	37.70	non-plastic	57.04	1.04	Silty sand (SM)
improved panel (IP)	8.85-9.00	26.03	non-plastic	20.92	1.46	Silty sand (SM)
improved panel (IP)	9.80-10.00	4.77	non-plastic	2.56	1.32	Poorly graded sand (SP)
improved panel (IP)	10.35-10.55	40.94	non-plastic	-	-	Silty sand (SM)*
improved panel (IP)	11.80-12.00	28.38	non-plastic	-	-	Silty sand (SM)*
improved panel (IP)	12.40-12.60	1.40	non-plastic	2.27	1.15	Poorly graded sand (SP)

Notes: FC is the fines content; *PI* is the plasticity index; C_U is the coefficient of uniformity; C_C is the coefficient of gradation; * refers to USCS visual manual procedure.

Table 3. Average geotechnical parameters estimated by CPTU and SDMT in natural (NS) and treated (TS) soils. The percentage in brackets represents the increase of the average parameters that was due to the improvement and is equal to the difference between the TS and NS parameters divided by the NS parameter multiplied by 100%.

z (m)	*Soil*	CPTU		DMT		CPTU-DMT			SDMT
		q_t (MPa)	D_R (%)	K_D (-)	M (MPa)	M/q_t (-)	OCR (-)	K_0 (-)	V_S (m/s)
4.0-7.0	NS	7.10	53.91	8.45	70.96	10.39	2.11	0.70	154
	TS	9.21 (30%)	60.87 (13%)	12.49 (48%)	128.31 (80%)	13.43 (29%)	3.18 (51%)	0.91 (29%)	179 (16%)
7.0-9.0	NS	9.96	58.36	8.48	94.91	7.42	1.11	0.51	181
	TS	13.44 (35%)	66.28 (14%)	12.98 (53%)	177.16 (87%)	14.37 (94%)	3.53 (218%)	0.99 (93%)	178 (-2%)

Table 4. Comparison of liquefaction severity indices obtained from CPTU in pre-blast natural (NS) and treated (TS) soils for both the ground motions. The percentage in brackets represents the variation of the average parameters that was due to the improvement and is equal to the difference between the TS and NS parameters divided by the NS parameter multiplied by 100%.

		M_w = 5.9, PGA = 0.29g				M_w = 6.14, PGA = 0.22g			
Method	*Soil*	*LPI*	*LPIish*	*LSN*	*S (cm)*	*LPI*	*LPIish*	*LSN*	*S (cm)*
Robertson and Wride (1998)	NS	4.020	1.416	13.027	6.485	1.695	0.106	8.352	3.977
	TS	1.573 (-61%)	0.401 (-72%)	5.711 (-56%)	2.284 (-65%)	0.903 (-47%)	0.026 (-75%)	4.207 (-50%)	1.591 (-60%)
Idriss and Boulanger (2008)	NS	4.616	0.802	11.653	6.133	1.145	0.178	6.101	3.086
	TS	1.925 (-58%)	0.408 (-49%)	6.464 (-45%)	2.910 (-53%)	0.737 (-36%)	0.000 (-100%)	3.321 (-46%)	1.404 (-55%)
Idriss and Boulanger (2008) with FC_{Lab}	NS	1.411	0.668	3.480	1.678	0.701	0.262	2.224	1.077
	TS	0.925 (-34%)	0.243 (-64%)	2.245 (-35%)	0.995 (-41%)	0.399 (-43%)	0.000 (-100%)	1.335 (-40%)	0.626 (-42%)
Boulanger and Idriss (2014)	NS	18.700	11.664	24.034	13.809	12.570	6.289	22.166	12.446
	TS	10.668 (-43%)	5.088 (-56%)	16.440 (-32%)	8.388 (-39%)	5.637 (-55%)	1.726 (-72%)	12.756 (-42%)	6.213 (-50%)
Boulanger and Idriss (2014) with FC_{Lab}	NS	4.295	2.299	7.694	3.750	2.439	1.030	5.417	2.631
	TS	2.434 (-43%)	0.939 (-58%)	4.560 (-41%)	2.083 (-44%)	1.103 (-55%)	0.482 (-53%)	2.965 (-45%)	1.367 (-48%)

Fig. 1

Click here to access/download;Figure;Fig.1.tif

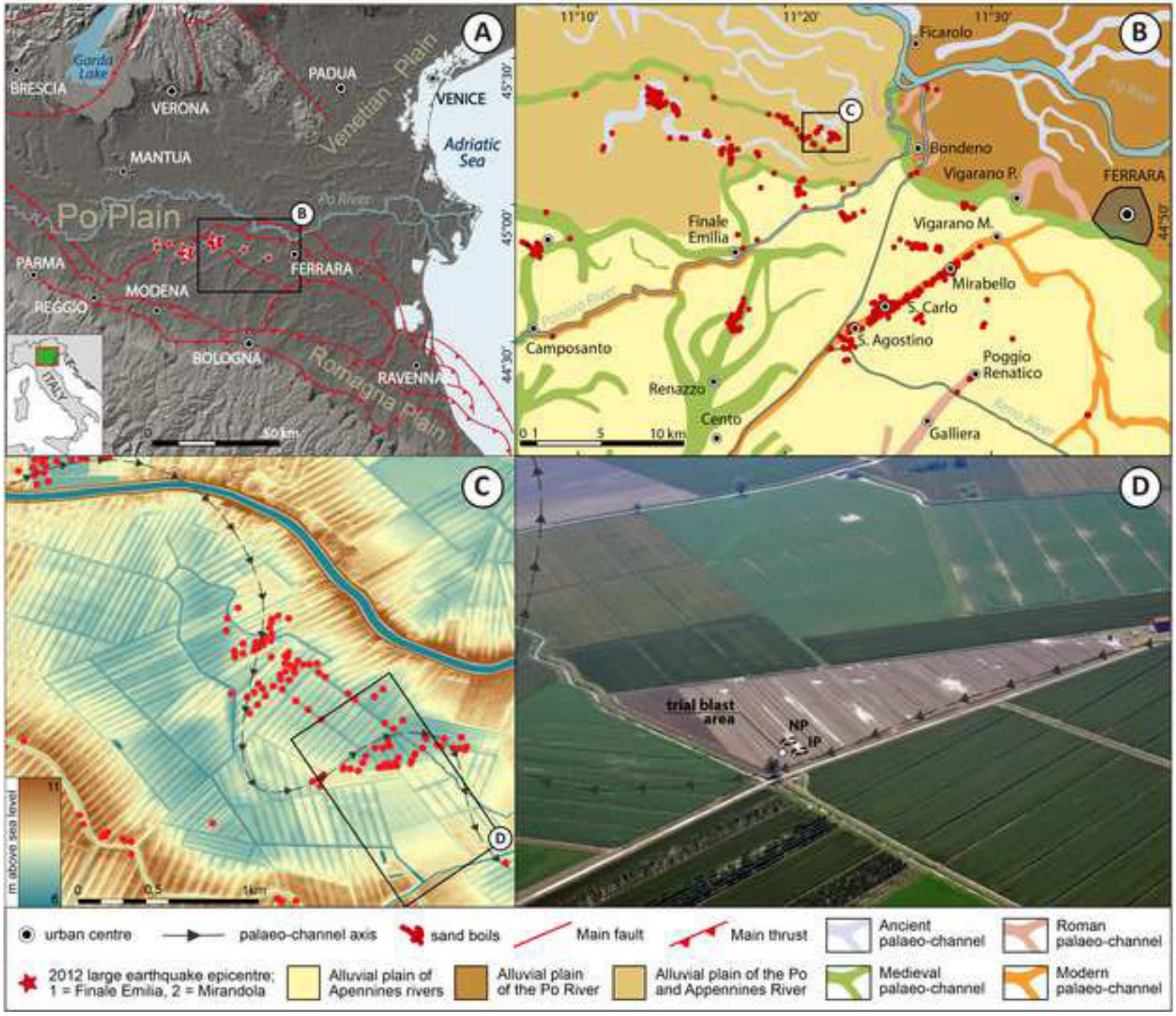

Fig. 2

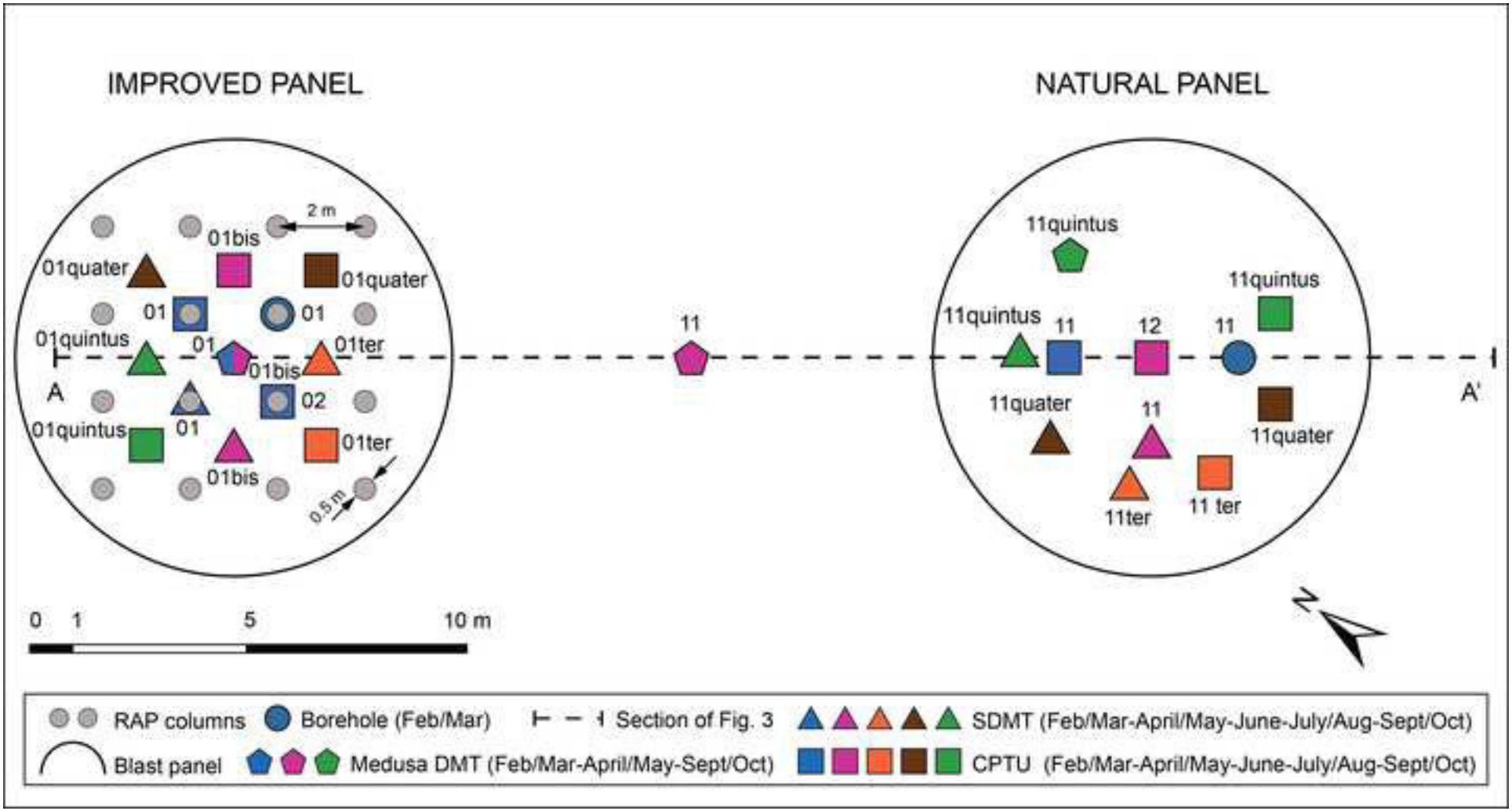

Fig. 3

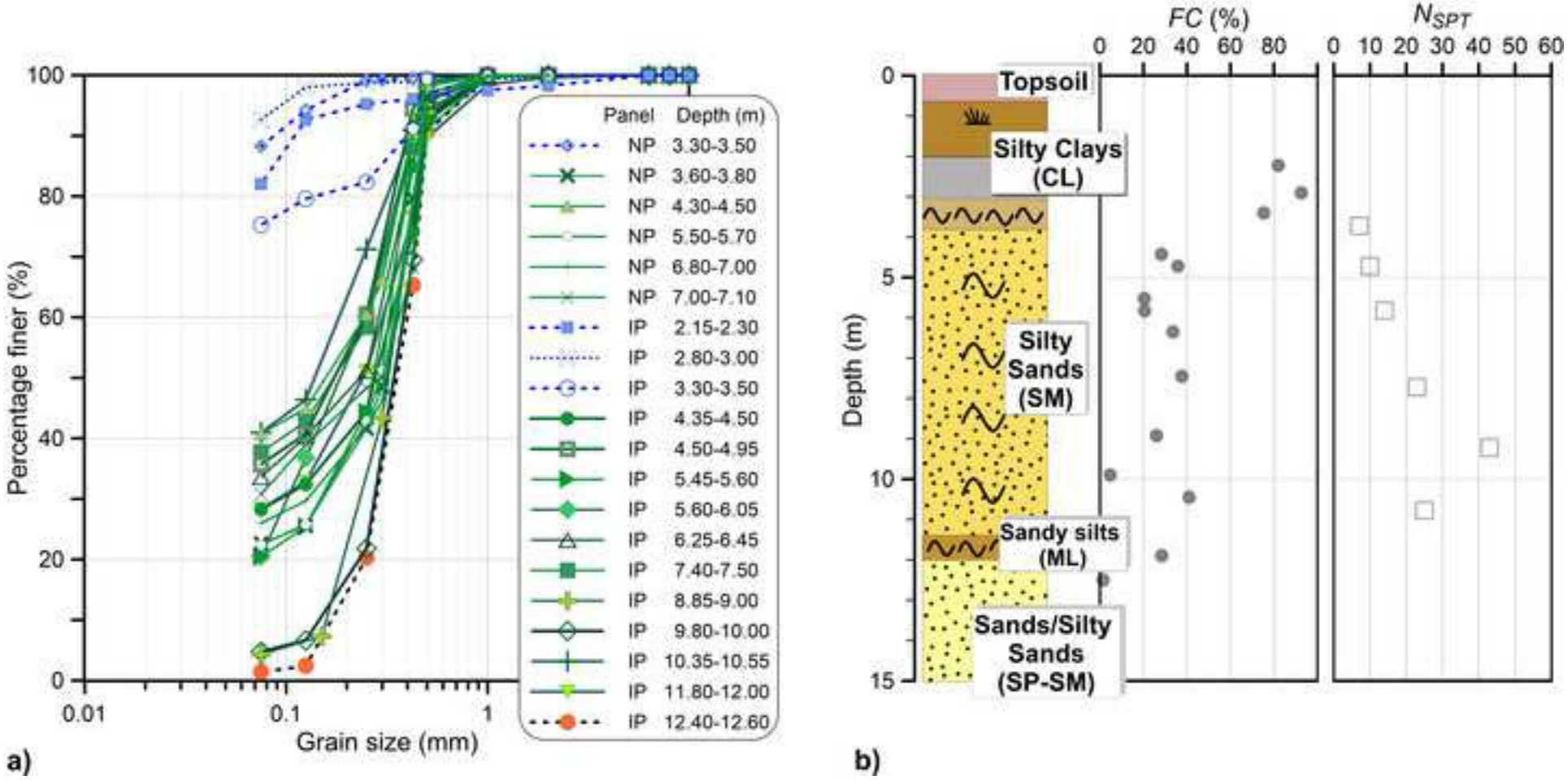

Fig. 4

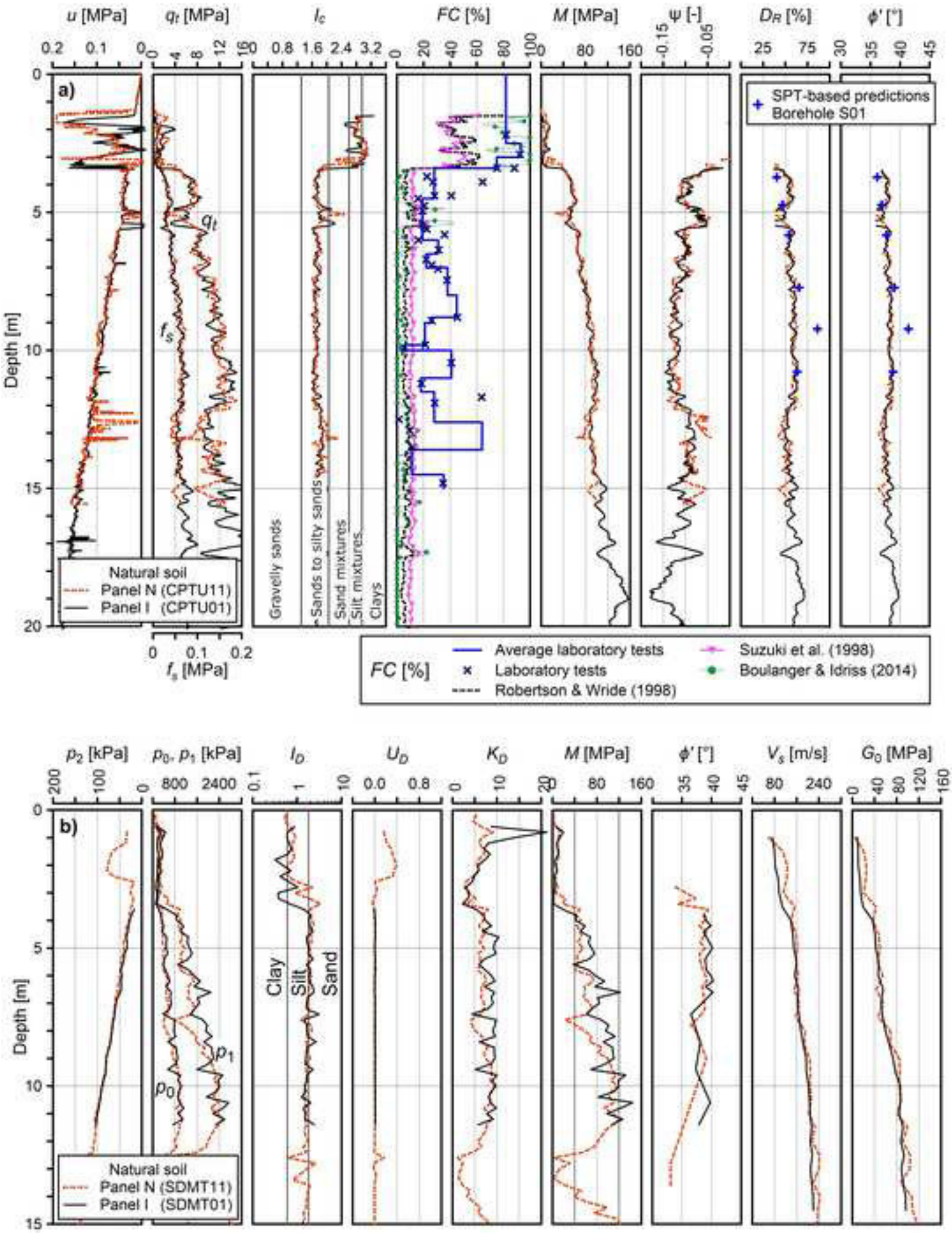

Fig. 5

Click here to access/download;Figure;Figure 5.tiff

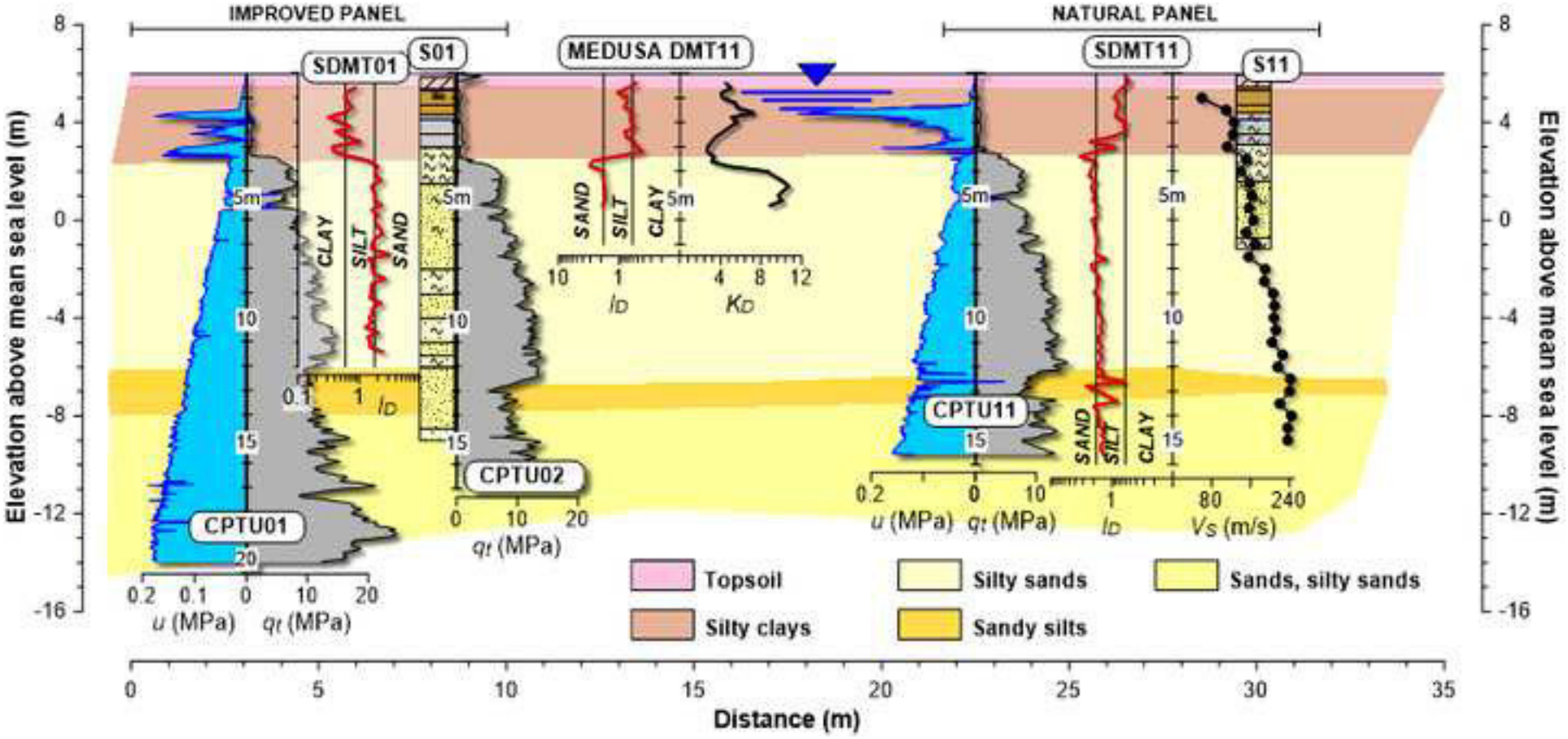

Fig. 6

Click here to access/download;Figure;Fig. 6.tif

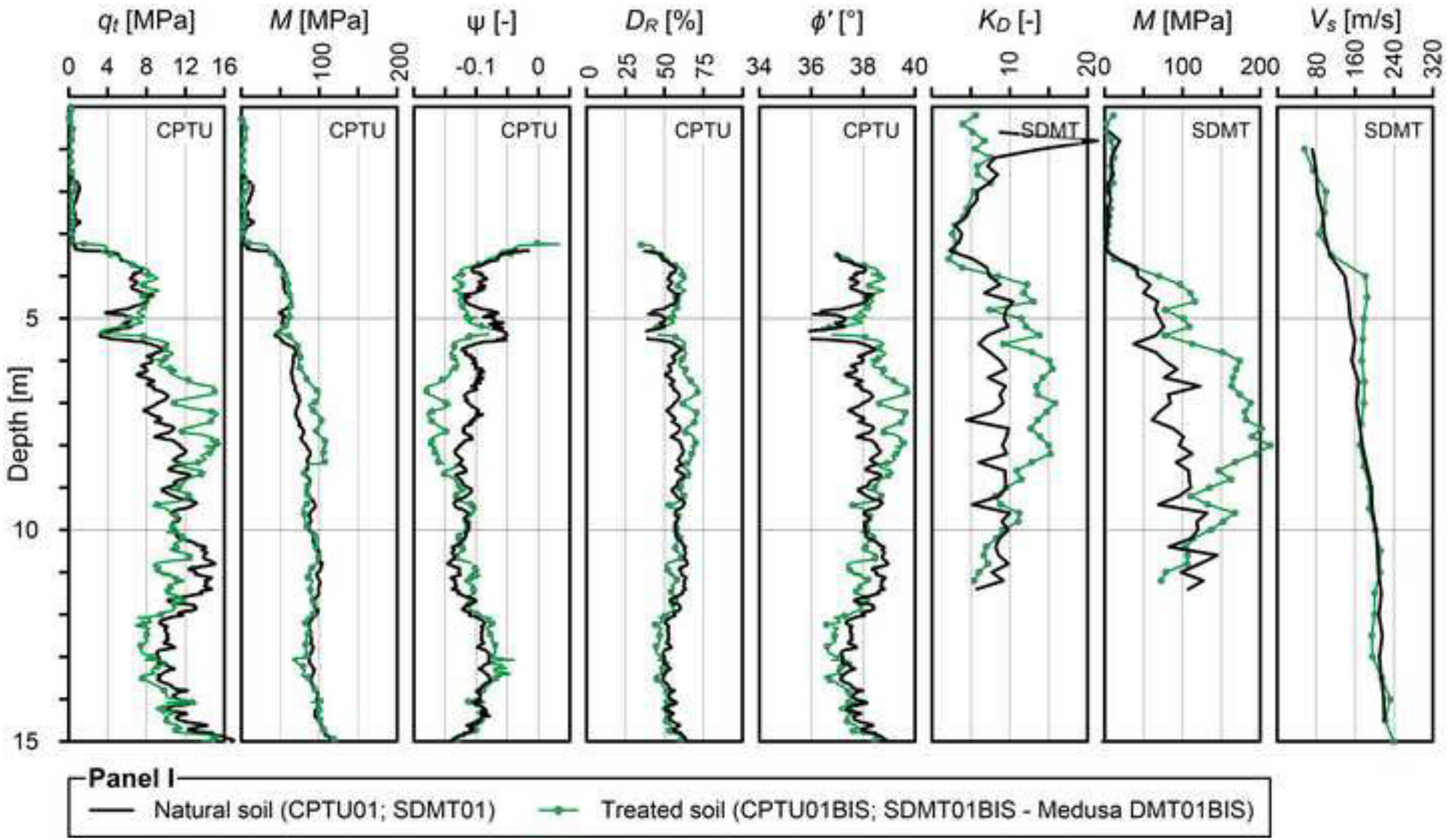

Fig. 7

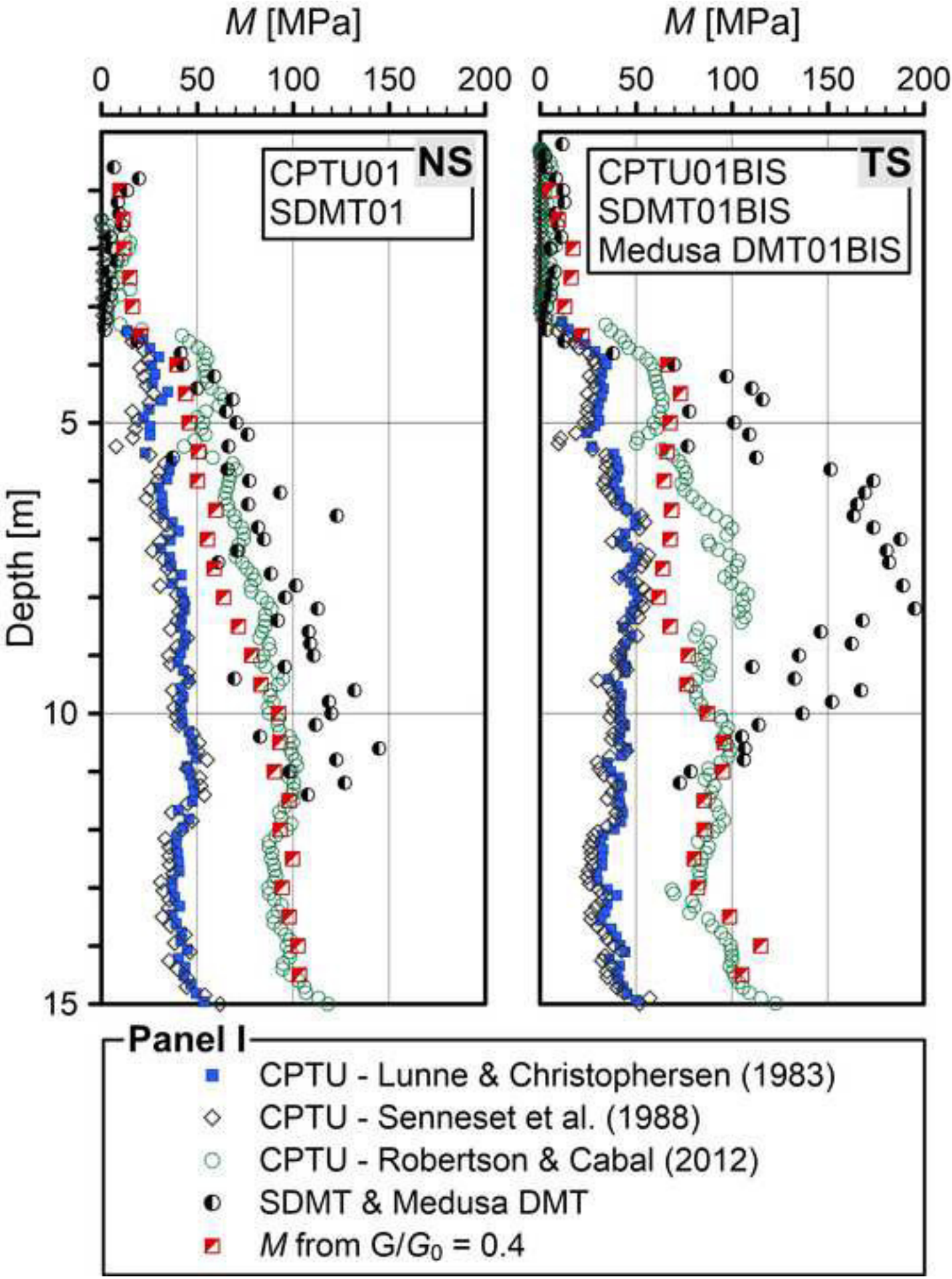

Fig. 8

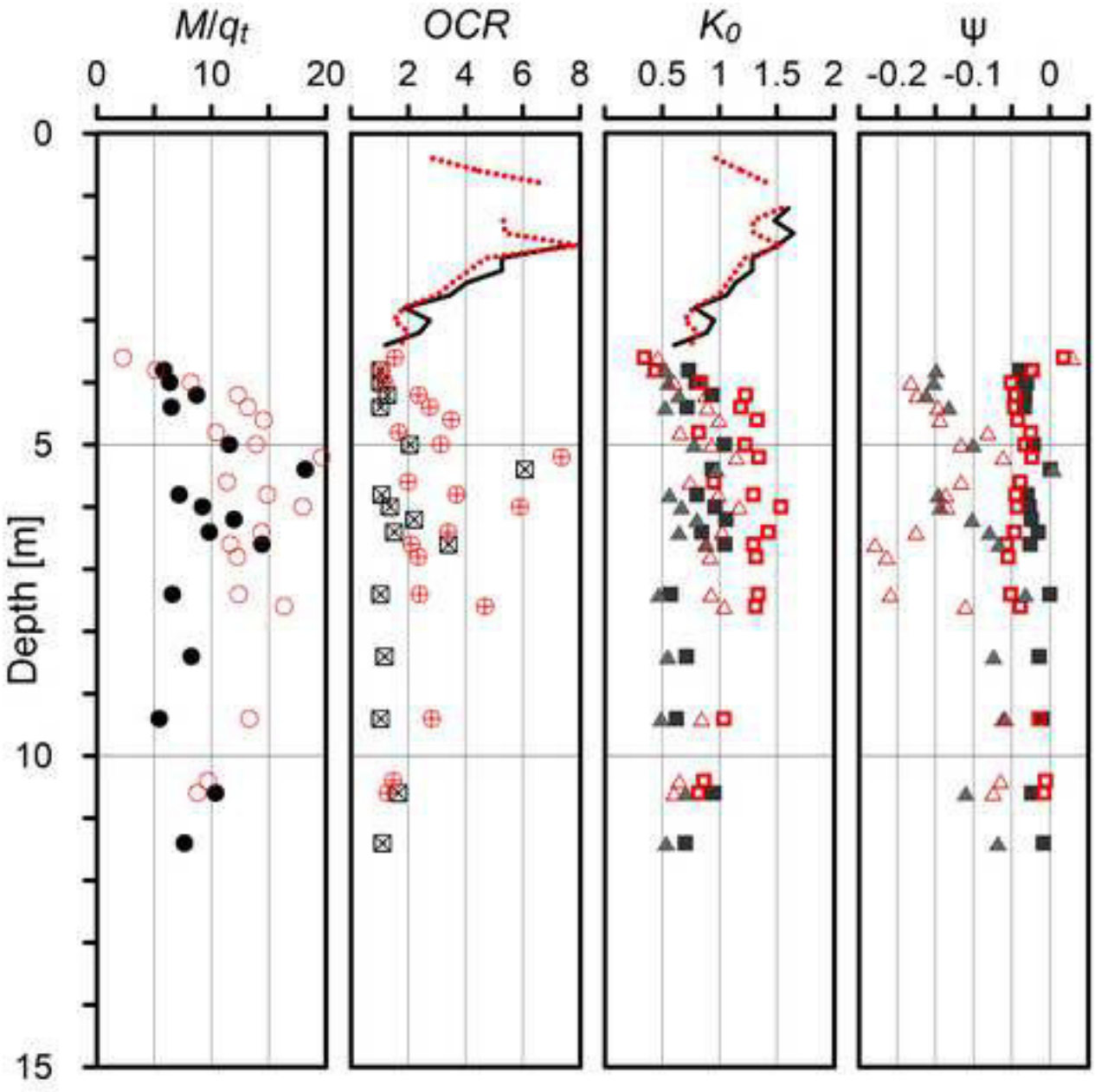

Panel I

M/qt
- ● Natural (N): SDMT01 & CPTU01
- ○ Treated (T): SDMT01BIS + Medusa DMT01BIS & CPTU01BIS

OCR
- — N ····· T Marchetti (1980)
- ⊠ N ⊕ T Monaco et al. (2014)

K0
- — N ····· T Marchetti (1980)
- ■ N ▫ T Baldi et al. (1986)
- ▲ N △ T Hossain & Andrus (2016)

ψ
- ■ N ▫ T Baldi et al. (1986); Yu (2004)
- ▲ N △ T Hossain & Andrus (2016); Yu (2004)

Fig. 9

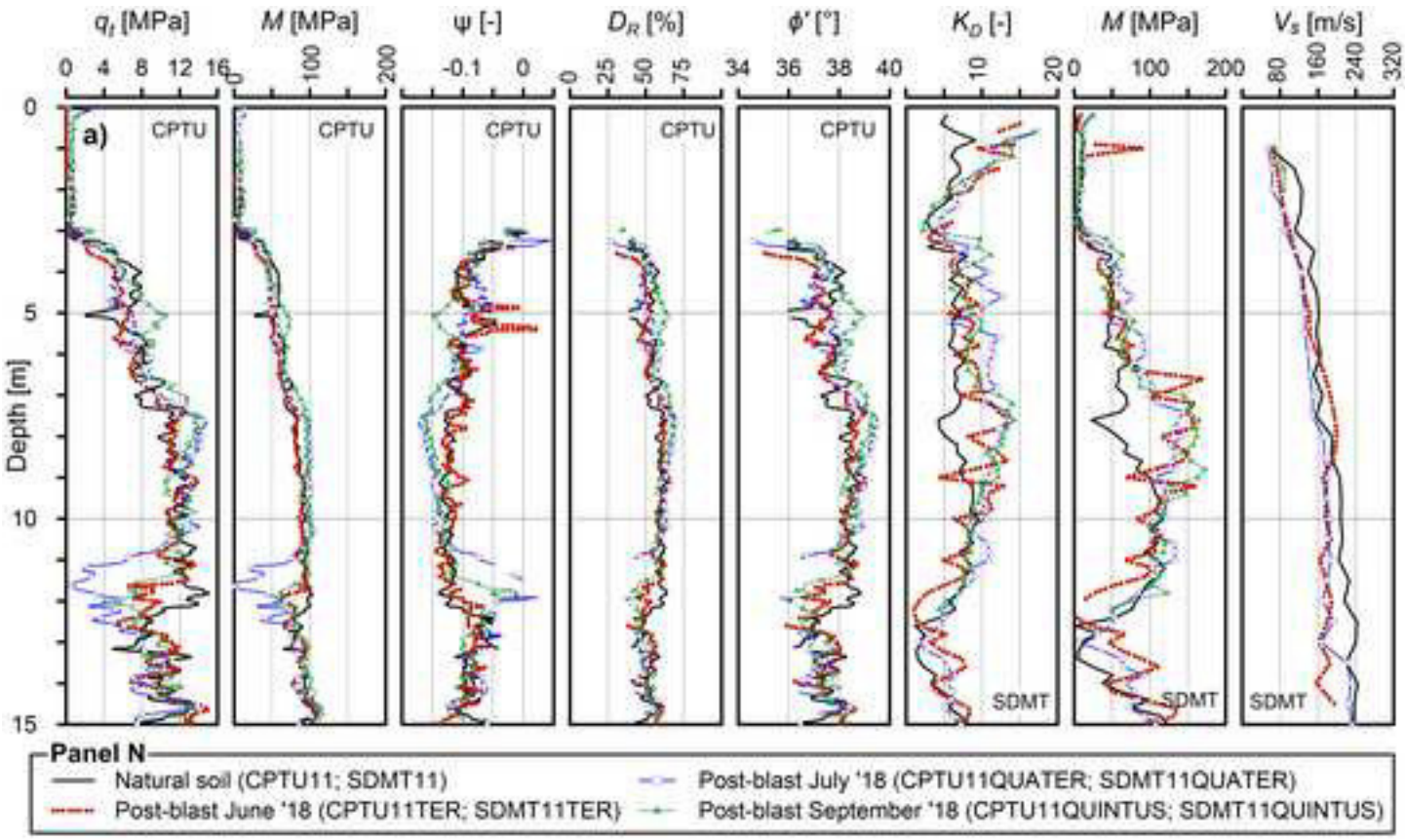

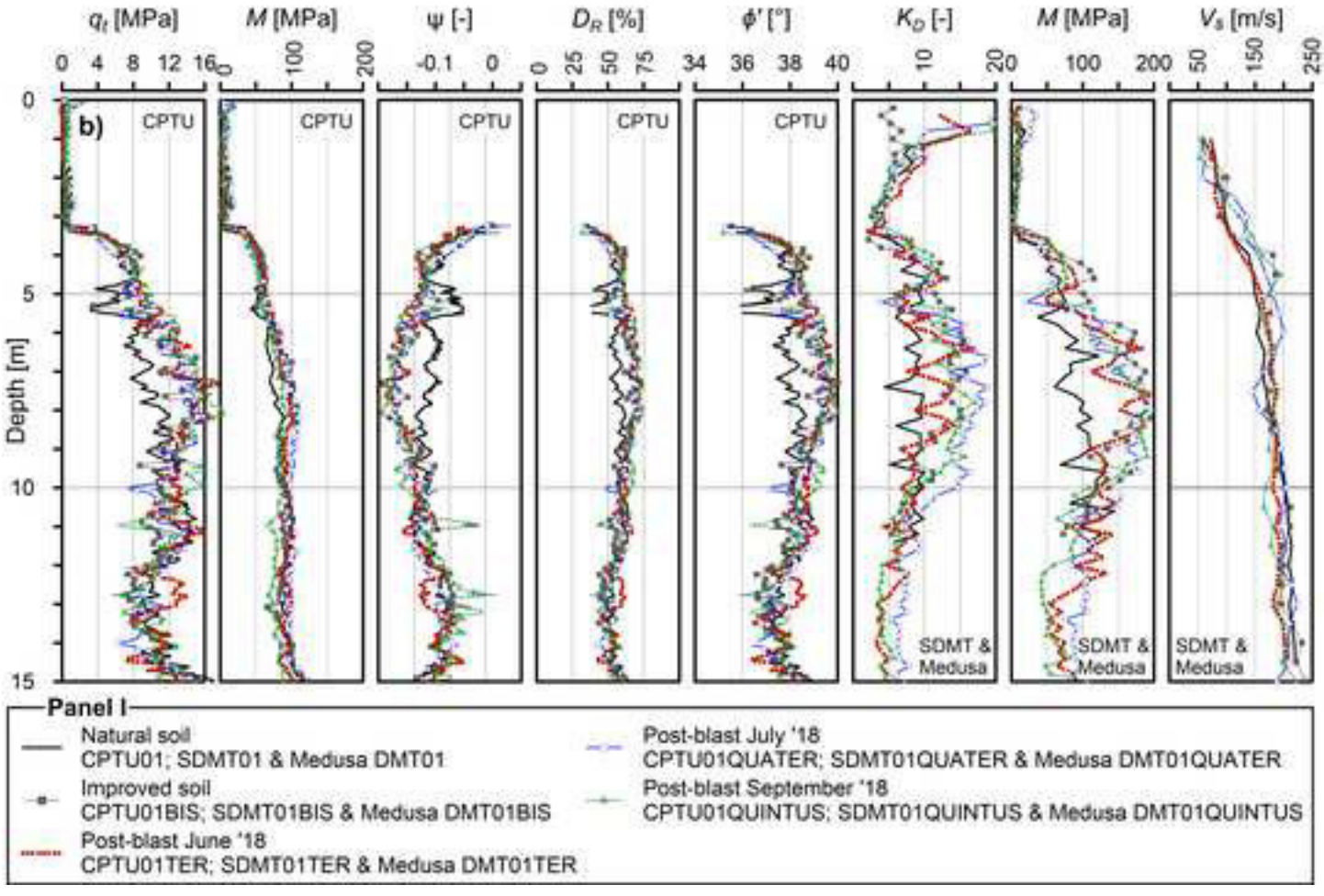

Fig. 10

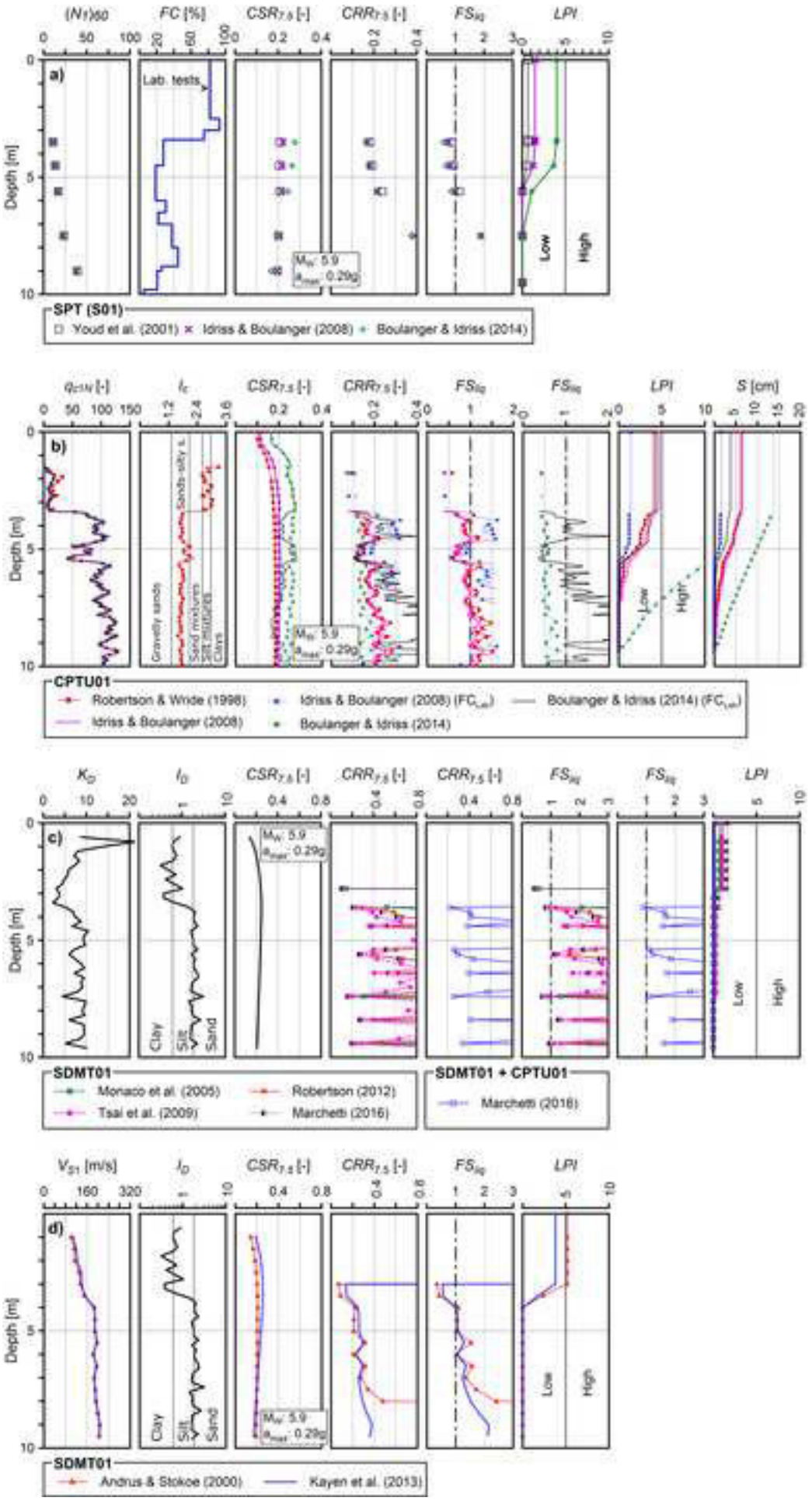

Fig. 11

Click here to access/download;Figure;Figure 11.tif

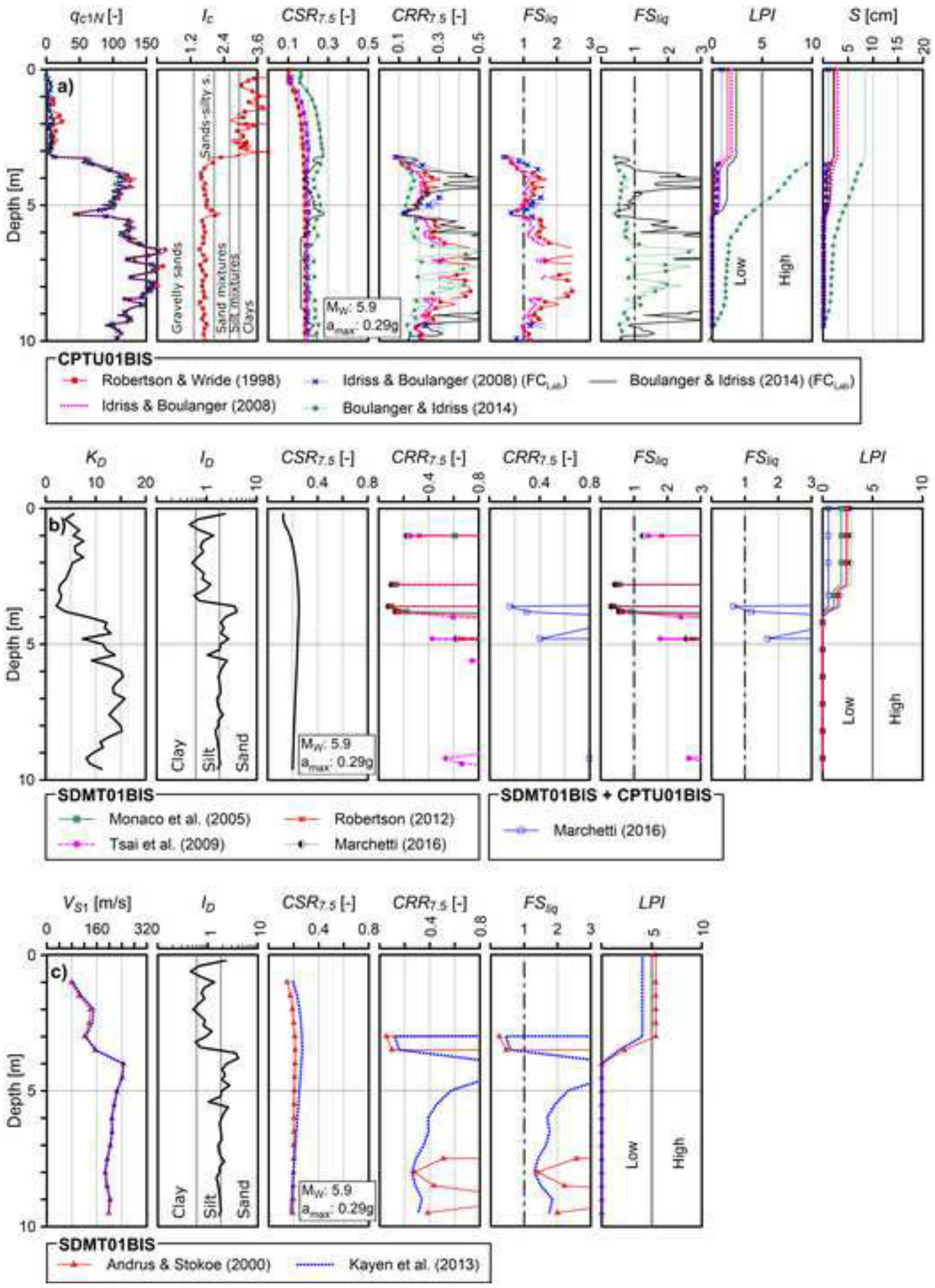

List of Figures

Fig. 1. (a) Location of the Bondeno Test Site (BTS) and of 2012 main shocks; (b) map of the paleochannel bodies (modified after Stefani et al. 2018), of the surface manifestations of liquefaction following the 2012 Emilia-Romagna earthquake (Emergeo Working Group 2013) and of the location of the blast area; (c) geomorphological features from LIDAR map (modified after Amoroso et al. 2020): greenish color indicates lower elevation above the sea level, while brownish color refers to higher elevation; (d) aerial photo with liquefaction evidences (modified after EMERGEO Working Group 2013).

Fig. 2. Map of the in-situ tests carried out at the BTS pre-blast (February–March 2018), post-RAP (April 2018) and post-blast (June, July–August and September 2018).

Fig. 3. (a) Grain size analyses; (b) borehole log, SPT blow count (N_{SPT}) and fines content (FC) profiles.

Fig. 4. CPTU and SDMT results in natural soils pre-blast (NP and IP pre-RAP): (a) u, q_t-f_s, I_c, FC, M, ψ, D_R, φ' from CPTU; (b) p_2, p_0-p_1, I_D, U_D, K_D, M, φ', V_S, G_0 from SDMT.

Fig. 5. North-South cross-section of the BTS with "first-phase" CPTU and SDMT log profiles and boreholes.

Fig. 6. CPTU and SDMT interpreted results in natural (NS) and treated (TS) soils: q_t, M, ψ, D_R, φ' from CPTU; K_D, M, V_S from SDMT.

Fig. 7. Comparison of the constrained modulus profiles in natural (NS) and treated (TS) soils obtained from CPTU and SDMT (IP pre- and post-RAP).

Fig. 8. CPTU-DMT combined interpreted results in natural (NS) and treated (TS) soils: M/q_t, OCR, K_0, ψ.

Fig. 9. CPTU and SDMT interpreted results in (a) natural soil pre- and post-blast (NP) and (b) treated soil pre and post-blast (IP): Q_t, M, D_R, φ' from CPTU; K_D, M, V_S from SDMT.

Fig. 10. Liquefaction assessment in natural soil (NS) pre-blast by (a) SPT, (b) CPTU, (c) DMT and combined CPTU-DMT, (d) V_S test results.

Fig. 11. Liquefaction assessment in treated soil (TS) pre-blast by (a) CPTU, (b) DMT and combined CPTU-DMT, (c) V_S test results.